ORIGINAL ARTICLE



Exploring within-plant hydraulic trait variation: A test of the vulnerability segmentation hypothesis

Jean V. Wilkening^{1,2,3} □ | Robert P. Skelton^{4,5} □ | Xue Feng^{2,3} □ | Todd E. Dawson⁶ □ | Sally E. Thompson^{7,8} □

¹Civil and Environmental Engineering, University of California, Berkeley, Berkeley, California, USA

²Civil, Environmental, and Geo- Engineering, University of Minnesota, Minneapolis, Minnesota, USA

³St. Anthony Falls Laboratory, University of Minnesota, Minneapolis, Minnesota, USA

⁴South African Environmental Observation Network, Cape Town, South Africa

⁵School of Animal, Plant and Environmental Sciences, University of the Witwatersrand, Johannesburg, South Africa

⁶Integrative Biology, University of California, Berkeley, Berkeley, California, USA

⁷Civil, Environmental, and Mining Engineering, University of Western Australia, Perth, Western Australia, Australia

⁸Centre for Water and Spatial Science, University of Western Australia, Perth, Western Australia, Australia

Correspondence

Jean V. Wilkening, Civil and Environmental Engineering, University of California, Berkeley, Berkeley, CA, USA.

Email: jvwilkening@berkeley.edu

Funding information

National Science Foundation; Royal Society; African Academy of Sciences

Abstract

Observations show vulnerability segmentation between stems and leaves is highly variable within and between environments. While a number of species exhibit conventional vulnerability segmentation (stem P_{50} < leaf P_{50}), others exhibit no vulnerability segmentation and others reverse vulnerability segmentation (stem P₅₀> leaf P_{50}). We developed a hydraulic model to test hypotheses about vulnerability segmentation and how it interacts with other traits to impact plant conductance. We do this using a series of experiments across a broad parameter space and with a case study of two species with contrasting vulnerability segmentation patterns: Quercus douglasii and Populus trichocarpa. We found that while conventional vulnerability segmentation helps to preserve conductance in stem tissues, reverse vulnerability segmentation can better maintain conductance across the combined stem-leaf hydraulic pathway, particularly when plants have more vulnerable P_{50} s and have hydraulic segmentation with greater resistance in the leaves. These findings show that the impacts of vulnerability segmentation are dependent upon other plant traits, notably hydraulic segmentation, a finding that could assist in the interpretation of variable observations of vulnerability segmentation. Further study is needed to examine how vulnerability segmentation impacts transpiration rates and recovery from water stress.

KEYWORDS

cavitation, hydraulic model, hydraulic segmentation, plant hydraulics, vulnerability segmentation

1 | INTRODUCTION

Vegetation moderates the global water, carbon and energy balances. Yet vegetation worldwide is expected to experience more intense and frequent water stress in the future, as climate change increases drought frequency and severity (Williams et al., 2022). Water stress can impair plant function, reduce productivity and growth and contribute to plant mortality (Choat et al., 2018; McDowell et al., 2008). Changing plant function and/or ecosystem composition through plant mortality can therefore alter ecosystem function, water resources and the climate itself (Bonan, 2008).

This is an open access article under the terms of the Creative Commons Attribution License, which permits use, distribution and reproduction in any medium, provided the original work is properly cited.

© 2023 The Authors. Plant, Cell & Environment published by John Wiley & Sons Ltd.

3653040, 2023,

Plant drought response arises from the interplay of the physical environment with plant physiological traits (Feng et al., 2018; Kannenberg et al., 2022). Plant hydraulics-the variable characteristics of roots, xylem and stomata as water conduits within the soilplant-atmosphere system-provides a useful framework for understanding and predicting plant-water interactions under varying environmental conditions (Sperry & Love, 2015). Plant hydraulic theory describes the movement of water as flow under tension through xylem, driven by gradients in water potential from root to leaf (Dixon & Joly, 1894). As water potentials in xylem become more negative, metastable water within the xylem may form air bubbles (emboli) that can lead to cavitation in the hydraulic pathway. Emboli block flow in affected xylem, reducing plant hydraulic conductance (Tyree et al., 1994). Xylem cavitation is an important driver of drought mortality (Choat et al., 2018; McDowell et al., 2008). Vulnerability to embolism varies widely across species (Anderegg et al., 2016). Vulnerability is commonly characterised by P₅₀ values, which define the water potential at which cavitation causes a 50% loss of conductance, relative to unimpaired xylem. More negative P_{50} values indicate less vulnerable (safer) xylem and less negative P_{50} values indicate greater vulnerability to embolism. Given the consequences of xylem cavitation, many plants have hydraulic traits that minimise cavitation risk, while balancing other potential tradeoffs (e.g., decreased growth rates and/or hydraulic efficiency) (Cochard & Delzon, 2013; Eller et al., 2018; Gleason et al., 2016; Sperry, 2003).

Zimmermann (1983) proposed that plants which concentrated embolism in distal tissues (e.g., leaves vs. stems) would experience a lower 'cost' of embolism than plants which experienced cavitation in central stem tissues. Leaves in these plants, he hypothesised, would function like 'fuses' or 'safety valves', protecting stem xylem from cavitation. For leaf xylem to provide this function requires hydraulic differentiation of stem and leaf xylem—a 'segmentation' of hydraulic properties between tissues. Zimmermann (1978, 1983) proposed that leaf xylem with lower hydraulic conductance than stem xylem would create such segmentation by requiring greater water potential gradients (and thus lower leaf water potentials) to move water through low conductance leaf hydraulic pathways. The resulting lower water potentials in the distal sections/tissues would then preferentially induce embolism in leaves. This segmentation in hydraulic conductance is referred to as 'hydraulic segmentation'.

Tyree and Ewers (1991) expanded Zimmermann's Segmentation Hypothesis, by highlighting that less negative P_{50} in leaf than stem xylem would also enable leaves to function as safety valves for cavitation. This distinction in P_{50} values between leaves and stems is referred to as 'vulnerability segmentation'. Hydraulic segmentation and vulnerability segmentation rely on different anatomical attributes, and are largely independent. Hydraulic segmentation is primarily driven by different conduit diameters, conduit density, and pit pore membrane properties between leaf and stem xylem (Zimmermann, 1982) and possibly by cell wall properties (e.g., density of cellulose microfibrils and lignin). Conversely, vulnerability to embolism is driven primarily by pit pore membrane properties (Levionnois et al., 2022). There is no clear, consistent relationship between conduit diameter and xylem vulnerability to droughtinduced embolism in major land plant lineages: a weak positive or no relationship between conduit diameter and vulnerability to droughtinduced embolism has been reported among conifers (e.g., Pittermann et al., 2006; Tyree et al., 1994, but see also Larter et al., 2017), angiosperms (e.g., Cochard et al., 1999; Hacke et al., 2005, but see also Hargrave et al., 1994; Martínez-Vilalta et al., 2002), and mixed compositions of conifer and angiosperm species (e.g., Davis et al., 1999; Tyree & Dixon, 1986). However, while hydraulic and vulnerability segmentation are distinct mechanisms, they are not mutually exclusive.

Methods to characterise embolism vulnerability in different tissues have advanced in capability and accessibility (e.g., Brodribb et al., 2016; Charra-Vaskou et al., 2012; Cochard et al., 2015; Holbrook et al., 2001; Nolf et al., 2015; Petruzzellis et al., 2020; Ponomarenko et al., 2014). In particular, measurement of leaf xylem vulnerability now enables the empirical quantification of vulnerability segmentation between stem and leaf tissues (Brodribb et al., 2017, 2016). Many studied species conform to the Vulnerability Segmentation Hypothesis, with leaf xylem more susceptible to embolism than stem xylem (leaf P_{50} > stem P_{50}) (Bucci et al., 2012; Charrier et al., 2018, 2016; Chen et al., 2009; Choat et al., 2005; Cochard et al., 1992; Hao et al., 2008; Hochberg et al., 2016, 2017; Johnson et al., 2011, 2016; Levionnois et al., 2020; Losso et al., 2019; Nolf et al., 2015; Rodriguez-Dominguez et al., 2018; Skelton et al., 2021, 2019, 2018; Smith-Martin et al., 2020; Song et al., 2022; Zhu et al., 2016). Because of its prevalence, we refer to the pattern of more vulnerable leaf xylem than stem xylem as conventional vulnerability segmentation. However, this pattern of vulnerability segmentation has been far from ubiquitous in the growing body of measurements of vulnerability segmentation.

Some species do not exhibit vulnerability segmentation (leaf P_{50} = stem P_{50}) (Bouche et al., 2016; Chen et al., 2009; Guan et al., 2022; Klepsch et al., 2018; Li et al., 2020; Losso et al., 2019; Nolf et al., 2015; Skelton et al., 2021, 2017, 2018; Smith-Martin et al., 2020; Zhu et al., 2016), and, other species display stem xylem that are more vulnerable to embolism than are leaf xylem (leaf P₅₀< stem P₅₀) (Klepsch et al., 2018; Levionnois et al., 2020; Villagra et al., 2013; Zhu & Cao, 2009; Zhu et al., 2015, 2016). We refer to this pattern as reverse vulnerability segmentation. Further details of published observations of reverse vulnerability segmentation are summarised in Supporting Information: Table S1. While the number of observations of reverse vulnerability segmentation remain relatively small, and indeed the overall number of species for which vulnerability segmentation pattern has been characterised is also relatively small, reverse vulnerability segmentation has been observed independently by different groups in various species using a variety of methods.

Understanding of reverse vulnerability segmentation is nascent, with observations still emerging to provide a sense of the overall prevalence of reverse vulnerability segmentation. One hypothesis suggests reverse vulnerability segmentation is associated with mesic environments (Zhu et al., 2016), yet species exhibiting reverse

13653040, 2023, 9, Downloaded

wiley.com/doi/10.1111/pce.14649 by UNIVERSITY OF MINNESOTA 170 WILSON LIBRARY, Wiley Online Library on [27/02/2024]. See the Terms

articles are governed by the applicable Creative Common

segmentation are sympatric with conventionally segmented species (Levionnois et al., 2020). This suggests environmental forcing alone is unlikely to explain segmentation differences. In the few studies examining how vulnerability segmentation impacts plant function and drought resistance, neither reverse segmentation nor interactions with other traits (including hydraulic segmentation and safety [P_{50}]) were explored (Blackman et al., 2019; Levionnois et al., 2021; Sperry & Love, 2015).

The vulnerability segmentation hypothesis proposes that under water scarce situations, plants without vulnerability segmentation or with reverse segmentation would be disadvantaged relative to plants exhibiting conventional segmentation. Plants experiencing reverse vulnerability segmentation would be expected to experience relatively greater hydraulic damage to the stem which could contribute to higher mortality rates. These expectations may be confounded when traits other than vulnerability segmentation vary between plants. Most directly, embolism formation is related to the hydraulic safety (P_{50}) of tissues. P_{50} is variable and frequently correlated with other plant traits (Bartlett et al., 2016; Gleason et al., 2016; Mursinna et al., 2018; Reich, 2014). Additionally, hydraulic segmentation may be present independently of vulnerability segmentation (Zimmermann, 1983).

Given the complex suite of trait combinations that could interact with vulnerability segmentation to produce beneficial or harmful outcomes for a plant, mechanistic modelling offers an attractive tool to assess the implications of vulnerability segmentation (conventional, reverse, or absent) for plant outcomes. As the empirical picture continues to develop regarding patterns and prevalence of vulnerability segmentation, a theoretical investigation can complement the empirical observations by elucidating what adaptive strategies might exist behind different vulnerability segmentation patterns. Such a theoretical exploration can help to both interpret empirical studies of vulnerability segmentation, as well as guide further studies across species and environments. To address this need, we develop a simple hydraulic modelling framework, and use it to test hypotheses about how vulnerability segmentation impacts conductance (both in the stem and across the composite stem-leaf pathway) in the context of diverse plant traits. We hypothesise that:

- Hypothesis I: Plants with conventional vulnerability segmentation will experience less conductance loss than plants with reverse vulnerability segmentation, independent of variation in hydraulic segmentation and safety.
- Hypothesis II: A greater magnitude of vulnerability segmentation leads to greater differences in conductance loss relative to a plant with no vulnerability segmentation, independent of variation in hydraulic segmentation and safety.

We examine these hypotheses using model experiments across a broad plant trait parameter space, and by considering two species with opposite patterns of vulnerability segmentation. Conductance loss is modelled and compared for the stem alone, and for the combined stem-leaf hydraulic pathway (referred to as 'composite'

conductance). The results are used to assess how different vulnerability segmentation patterns, in association with other traits, impact plant vulnerability and function.

2 | METHODS

We develop a hydraulic model to examine how vulnerability segmentation impacts hydraulic functioning. The model explicitly represents hydraulic differences between stems and leaves. It is otherwise minimalist in design, so that its results provide information about the first-order effects of vulnerability segmentation.

The model is steady-state, such that it does not consider the role of plant capacitance or a dynamic soil water balance. While such dynamic processes certainly play a role in plant drought response, the goal of this study is to understand the as of yet unexplored first-order interactions between vulnerability segmentation and other traits (safety and hydraulic segmentation) which are thought to directly control embolism formation. Given the diversity of plant traits, this exploration already presents a sizeable parameter space, so additional variables are kept to a minimum to maintain tractability. Additionally, while capacitance is being increasingly recognised as an important trait for plant drought response, far fewer measurements exist as compared to traits like P₅₀ (Kattge et al., 2020) and it is even less clear how plant capacitance characteristics are correlated with patterns of vulnerability segmentation, such that it is difficult to confidently parameterise capacitance over a broad range of values of the other traits explored in this study.

We next develop a framework to quantitatively characterise segmentation at tissue and whole-plant scales. We use this framework to test our hypotheses about the role of vulnerability segmentation in plant function. Finally, we use the model to interpret an empirical case study of two real species with opposite vulnerability segmentation patterns.

2.1 | Hydraulic model

We adapt the widely used (Sperry et al., 1998, 2002; Sperry & Love, 2015) representation of the soil-plant-atmosphere continuum as a series of resistors (Figure 1a), to include an explicit description of vulnerability segmentation, amending the model formulation from Feng et al. (2018). The model solves for steady-state transpiration, plant water potentials and leaf and stem xylem hydraulic conductance as a function of soil water potential. The water flux through the plant is the product of the point conductance and water potential gradient, integrated across the range in water potential in the stem or leaves:

$$E = -\int_{\psi_X}^{\psi_{L1}} k_{\text{stem}}(\psi) d\psi, \tag{1}$$

$$E = -\int_{\psi_{1,1}}^{\psi_{1,2}} k_{\text{leaf}}(\psi) d\psi. \tag{2}$$

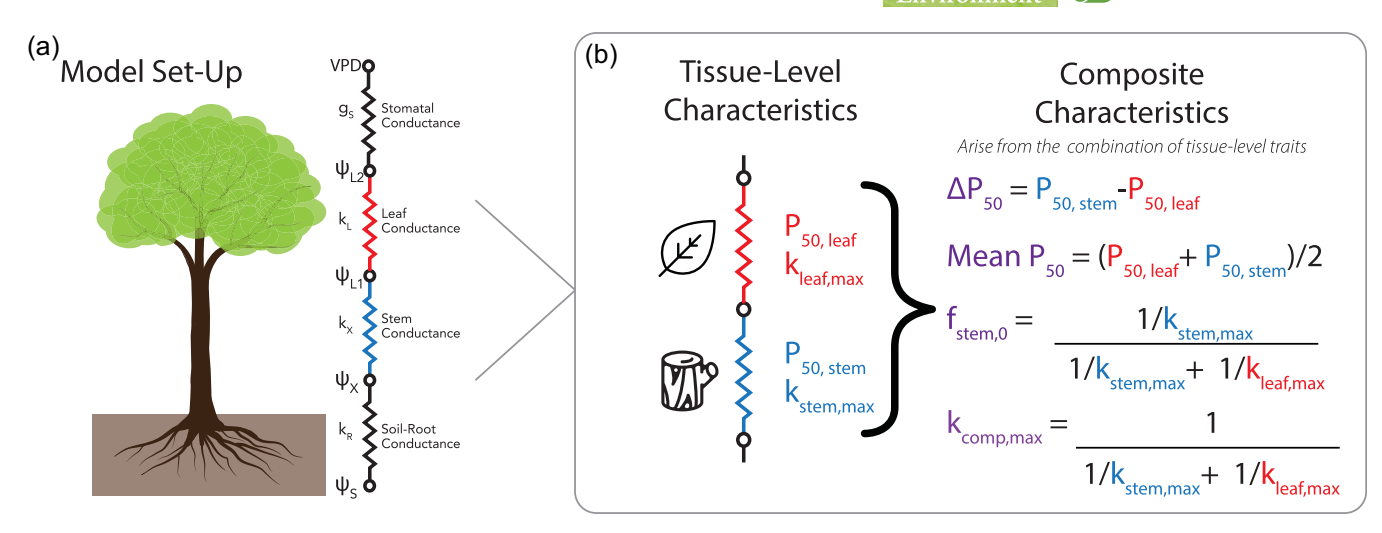


FIGURE 1 (a) Steady-state water transport is modelled using a series of variable resistors. Water is driven from soil to roots by the gradient between ψ_s and the xylem water potential (ψ_x) according to conductance k_r . Stem water transport is driven by the gradient between ψ_x and a proximal leaf water potential (ψ_{L1}) with a conductance of k_x . Water transport through the leaf is described by the leaf xylem hydraulic conductance k_L the gradient created between ψ_{L1} and a distal leaf water potential (ψ_{L2}). Water transport out of the stomata is then described according to the stomatal conductance (g_s) and the atmospheric vapour pressure deficit (VPD). (b) Within the plant, the hydraulic pathways through the stem and leaf xylem can be parameterised with respective P_{50} values and maximum initial conductances ($k_{\text{stem,max}}$ and $k_{\text{leaf,max}}$). From the individual tissue characteristics, other metrics are calculated to describe segmentation including the magnitude and direction of vulnerability segmentation (ΔP_{50}), the overall safety of the plant (mean P_{50}), the hydraulic segmentation ($f_{\text{stem,0}}$), and the composite stem-leaf conductance ($k_{\text{comp,max}}$).

Here E is the per-plant volumetric transpiration flux (m³ d⁻¹), ψ_X is the stem water potential (MPa), ψ_{L1} is the proximal leaf water potential at the stem-leaf transition (MPa), ψ_{L2} is the distal leaf water potential (MPa), k_{stem} is the stem conductance (m³ d⁻¹ MPa⁻¹], and k_{leaf} is the leaf xylem hydraulic conductance (k_{leaf}). The Kirchoff transform is used to describe and solve these equations in terms of matric flux potentials (ϕ_i) (Ross & Bristow, 1990; Sperry et al., 1998), where:

$$\phi_i = \int_{-\infty}^{\psi_i} k(\psi) d\psi. \tag{3}$$

With this description of matric flux potential, the transpiration flux through the plant can be described as:

$$E = -(\phi_{12} - \phi_{11}) = -(\phi_{11} - \phi_{x}). \tag{4}$$

The hydraulic conductances in stems and leaves are described as exponential sigmoidal functions of the water potentials in the respective tissues (Pammenter & Van der Willigen, 1998):

$$k_{\text{stem}}(\psi_X) = k_{\text{stem,max}} \left(1 - \frac{1}{1 + e^{(a\psi_X - P_{50,\text{stem}})}} \right),$$
 (5)

$$k_{\text{leaf}}(\psi_{L1}) = k_{\text{leaf,max}} \left(1 - \frac{1}{1 + e^{(a\psi_{L1} - P_{50,\text{leaf}})}} \right),$$
 (6)

where k_{max} is the maximum conductance in the tissue (m³ d⁻¹ MPa⁻¹), P_{50} is the water potential (MPa) at which there is a 50% loss of

conductivity in the tissue relative to the k_{max} , and a is a fitting parameter (-) describing the shape of the vulnerability curve. The water flux through stomata is described as:

$$E = -g_s(\psi)DV_w T_d A_L, \tag{7}$$

where $g_s(\psi)$ is the stomatal conductance varying with water potential ($mol\ H_2O\ m^{-2}\ s^{-1}$), D is the atmospheric vapour pressure deficit ($mol\ H_2O\ mol\ air^{-1}$), V_w is the molal volume of water ($m^3\ mol^{-1}$), T_d is daylength (s), and A_L is the total leaf area of the tree (m^2). The relationship between stomatal conductance and water potential in the leaf is described following Manzoni et al. (2014):

$$g_s(\psi_{L2}) = \max \left[g_{s,min}, g_{s,max} \left(1 - \frac{9}{10} \left(\frac{\psi_{L2}}{\psi_{90,s}} \right) \right) \right],$$
 (8)

where $g_{s,min}$ is the minimum stomatal conductance (including cuticular conductance) (mol H₂O m⁻² s⁻¹), $g_{s,max}$ is the maximum stomatal conductance (mol H₂O m⁻² s⁻¹), and $\psi_{90,s}$ is the leaf water potential at which there is 90% stomatal closure. The water uptake from the soil is calculated as:

$$E = -k_R(\psi_X - \psi_{\text{soil}}), \tag{9}$$

where k_R is the soil-root conductance (m³ d⁻¹ MPa⁻¹) and ψ_{soil} is the soil water potential (MPa). The model describes the value of k_R as constant fraction (x) of the soil to leaf resistance (Tyree & Sperry, 1988), such that k_R becomes a function of k_{stem} and k_{leaf} :

3653040, 2023, 9, Downlo

.com/doi/10.1111/pce.14649 by UNIVERSITY OF MINNESOTA 170 WILSON LIBRARY, Wiley Online Library on [27/02/2024]. See the Terms

$$k_{R} = \frac{\frac{1-x}{x}}{\frac{1}{k_{\text{stem}}(\psi_{X})} + \frac{1}{k_{|\text{eaf}}(\psi_{L})}}.$$
 (10)

Model parameters and variables are summarised in Table 1. The model assumes negligible changes in plant water storage. Given environmental conditions (ψ_{soil} and D) and plant traits, Equations (1), (2), (8) and (9) can be solved to give a steady-state transpiration rate, conductance in stem and leaf xylem, and plant water potentials.

2.2 | Characterising plants with segmentation

The model formulation treats plant stems and leaves as two resistors in series, with individual hydraulic conductances (k, or resistances, $R = k^{-1}$) and P_{50} values describing hydraulic safety (Figure 1b).

To quantify segmentation, it is helpful to define parameters describing tissue- and plant-level characteristics of plants exhibiting segmentation accounting for both the absolute value of the conductance and vulnerability in the plant, and for the distinctions between the stem and leaves in terms of conductance and vulnerability.

At the plant level, we define the 'true' composite stem-leaf conductance k_{comp} using the definition for resistors in series:

$$\frac{1}{k_{\text{comp}}} = \frac{1}{k_{\text{stem}}} + \frac{1}{k_{\text{leaf}}}.$$
 (11)

The maximum conductance before embolism ($k_{comp,max}$) is a fixed plant trait, but k_{comp} varies as soil water potentials decline. Because k varies with the changing water potential within each tissue, k_{stem} and k_{leaf} are computed using the maximum water potential in the respective tissues at a given ψ_{soil} and D. Unlike conductance, plant-level vulnerability for a plant exhibiting vulnerability segmentation cannot be simply defined, yet a reference value that encompasses both stem and leaf P_{50} is still valuable for this framework to be able to compare plants with similar vulnerability but potentially differing arrangements of vulnerability between tissues. We therefore characterise plant-level vulnerability as simply as possible, as the mean of the two P_{50} values:

Mean
$$P_{50} = \frac{P_{50,\text{stem}} + P_{50,\text{leaf}}}{2}$$
. (12)

Mean P_{50} represents the hypothetical plant-level vulnerability in a plant without vulnerability segmentation ($P_{50,\text{stem}} = P_{50,\text{leaf}}$). For plants with vulnerability segmentation, the mean P_{50} describes an intermediate hydraulic safety value relative to P_{50} values in individual tissues. However, this is used simply as a reference point derived from plant traits and does not describe the water potential when the whole plant will functionally lose 50% of its conductance, which instead comes from the model.

To describe differences in hydraulic conductance between stem and leaf tissues, the electrical circuit analogy is again useful. For mathematical convenience, resistances R = 1/k are used. The fraction of total resistance in the plant associated with the stem f_{stem} is defined as:

$$f_{\text{stem}} = \frac{R_{\text{stem}}}{R_{\text{stem}} + R_{\text{leaf}}} = \frac{\frac{1}{k_X}}{\frac{1}{k_X} + \frac{1}{k_I}}.$$
 (13)

An $f_{\rm stem}$ value of 0.5 indicates equal resistance (and conductance) in the stem and leaves. Values greater than 0.5 indicate greater relative hydraulic resistance in the stem than the leaves, and values less than 0.5 indicate greater relative hydraulic resistance in the leaves than the stem. While $f_{\rm stem}$ could be considered dynamically as conductances change with declines in water potential, we describe hydraulic segmentation with the initial value before any embolism ($f_{\rm stem,0}$), calculated using the initial, maximum tissue conductance values.

To describe vulnerability segmentation, we use the difference (ΔP_{50}) in P_{50} between stem and leaves:

$$\Delta P_{50} = P_{50,leaf} - P_{50,stem},$$
 (14)

which captures the magnitude and direction of vulnerability segmentation. Negative values of ΔP_{50} indicate reverse segmentation, and positive values indicate conventional segmentation. Larger absolute values of ΔP_{50} indicate greater magnitudes of vulnerability segmentation.

By combining these three metrics it is possible to consider, for example, how the behaviour of a hydraulically 'safe' plant (large negative mean P_{50}) with no vulnerability segmentation ($\Delta P_{50} \approx 0$) might vary in response to changing hydraulic segmentation (changing $f_{\text{stem},0}$). This framework allows us to isolate some features of segmentation for testing, while controlling others.

2.2.1 | Coordinated traits

Plant hydraulic, stomatal and vulnerability traits are often correlated (Gleason et al., 2016; Mursinna et al., 2018; Reich, 2014). Respecting these correlations when parameterising the hydraulic model is useful to reduce the parameter space and avoid assessing unrealistic plant trait combinations.

During parameterisation, the values of parameters describing segmentation, $f_{\text{stem,0}}$, ΔP_{50} , and mean P_{50} , are first set, assuming they are independent of one another. The remaining plant traits, $k_{\text{comp,max}}$, $k_{\text{stem,max}}$ and $k_{\text{leaf,max}}$, are then stochastically sampled to produce a large trait ensemble. Sampling is made from observed values (Kattge et al., 2020), with the distribution from which traits are sampled conditioned on the segmentation parameters used. Details of this procedure are presented in Supporting Information: Methods S1. This procedure enables testing of the hypotheses over a broad parameter space, while still being representative of potential trait coordination that exists in real plants.

TABLE 1 Variables and parameters used across all components of the model.

Symbol	Description	Dimensions	Units	Value/range					
	nental variables	Difficialons	Jiillo	. a.de, range					
D	Vapour pressure deficit – mol H_2O mol air ⁻¹ 0.033								
ψ_{soil}	Soil water potential	M L ⁻¹ T ⁻²	MPa	(-8.0, -1.0)					
	it parameters								
Independent parameters									
f _{stem,0}	Initial fraction of stem-leaf hydraulic resistance in stem	_	_	(0.1, 0.9)					
ΔP ₅₀	Difference in stem and leaf vulnerability	$M L^{-1} T^{-2}$	MPa	(-1.5, 1.5)					
P _{50,mean}	Mean of stem and leaf P ₅₀	$M L^{-1} T^{-2}$	MPa	(-6.5, -2.0)					
Coordinat	ted parameters (see Supporting Information: Methods S1)								
K_{sap}	Sapwood area specific hydraulic conductivity	Т	kg m $^{-1}$ s $^{-1}$ MPa $^{-1}$						
а	Vulnerability curve fitting parameter	-	-						
Н	Huber value	-	-						
Ψ _{90,S}	Leaf water potential at 90% stomatal closure	$M L^{-1} T^{-2}$	MPa						
Constant	/Calculated Parameters								
$k_{\rm stem, max}$	Maximum stem xylem conductance	$M^{-1} L^4 T$	$\mathrm{m^3~d^{-1}~MPa^{-1}}$	Supporting Information: Equation S4					
$k_{\text{leaf},\text{max}}$	Maximum leaf xylem conductance	$M^{-1} L^4 T$	$\mathrm{m^3~d^{-1}~MPa^{-1}}$	Supporting Information: Equation S5					
P _{50,leaf}	Water potential at 50% loss of leaf conductance	$M\ L^{-1}\ T^{-2}$	MPa	Supporting Information: Equation S2					
P _{50,stem}	Water potential at 50% loss of stem conductance	$M L^{-1} T^{-2}$	MPa	Supporting Information: Equation S1					
L _x	Canopy height	L	m	10.0					
A_L	Total leaf area	L ²	m ²	20.0					
$g_{s, min}$	Minimum stomatal conductance of water	M L ⁻² T ⁻¹	$\mathrm{mol}\;\mathrm{H_2O}\;\mathrm{m^{-2}}\;\mathrm{s^{-1}}$	$0.05 \times g_{s,\text{max}}$					
$g_{s, max}$	Maximum stomatal conductance of water	M L ⁻² T ⁻¹	$\mathrm{mol}\;\mathrm{H_2O}\;\mathrm{m^{-2}}\;\mathrm{s^{-1}}$	0.8					
X	Soil-root resistance fraction	-	-	0.18					
Model va	ariables								
Ε	Transpiration rate	L T ⁻¹	$\mathrm{m^3}~\mathrm{d^{-1}}$						
ψ_X	Xylem water potential	M L ⁻¹ T ⁻²	MPa						
k_R	Soil-root conductance	M^{-1} L^4 T	$\mathrm{m^3~d^{-1}~MPa^{-1}}$						
ψ_{L1}	Proximal leaf water potential	M L ⁻¹ T ⁻²	MPa						
ψ_{L2}	Distal leaf water potential	M L ⁻¹ T ⁻²	MPa						
k_{leaf}	Leaf xylem hydraulic conductance	$M^{-1} L^4 T$	m ³ d ⁻¹ MPa ⁻¹						
k_{stem}	Stem hydraulic conductance	M ⁻¹ L ⁴ T	m ³ d ⁻¹ MPa ⁻¹						
k_{comp}	Composite stem-leaf conductance	M ⁻¹ L ⁴ T	m ³ d ⁻¹ MPa ⁻¹						
g s	Stomatal conductance of water	M L ⁻² T ⁻¹	mol H ₂ O m ⁻² s ⁻¹						
Physical constants									
ρ_w	Density of water	M L ⁻³	kg m ⁻³	1000					
T _d	Day length (i.e., daylight)	T	S	36,000					
V_w	Molal volume of water	L ³ M ⁻¹	$\mathrm{m}^3~\mathrm{mol}^{-1}$	18e ⁻⁶					

(Continues)

TABLE 1 (Continued)

Symbol	Description	Dimensions	Units	Value/range			
Metrics from model output							
λ_{stem}	Conventional segmentation stem conductance advantage	-	%				
λ_{comp}	Conventional segmentation composite conductance advantage	-	%				
β	Composite hydraulic margin	$M\ L^{-1}\ T^{-2}$	MPa				
η	Prioritisation of stem conductance preservation	-	%				

Note: Values and/or ranges of parameters are shown where relevant. Further information on the constant parameter values is presented in Supporting Information: Table S1.

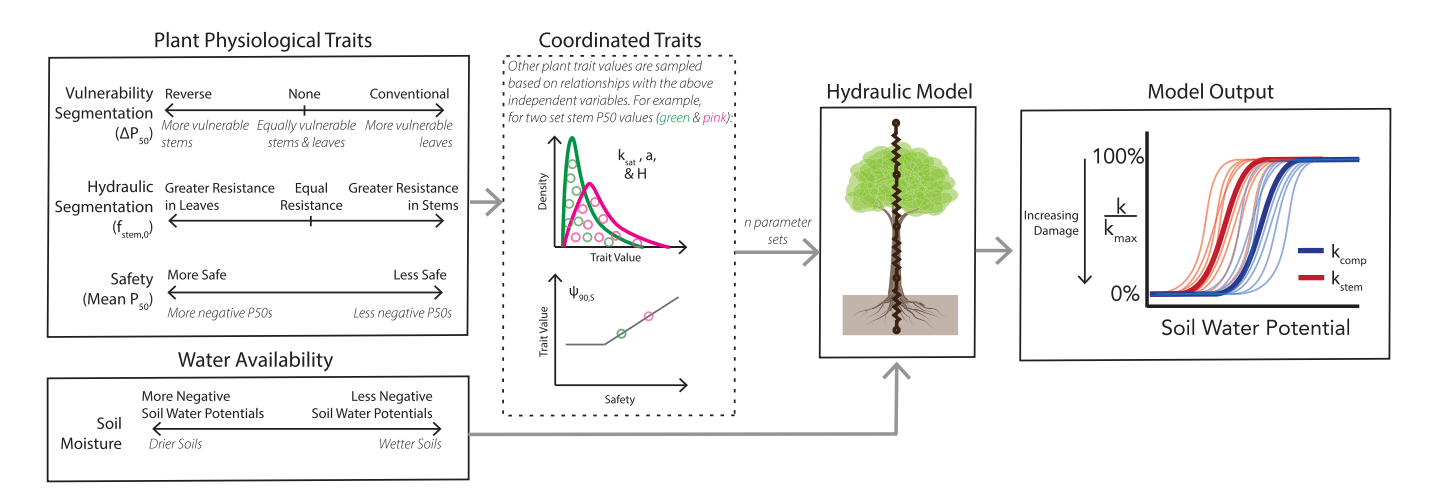


FIGURE 2 Three hydraulic traits are treated as independent: (i) Vulnerability segmentation, where plants can exhibit no segmentation, reverse or conventional segmentation, with varying magnitudes. (ii) Hydraulic segmentation, which varies depending on whether most hydraulic resistance in the plant is associated with stems or leaves, and (iii) Safety, represented by the spectrum of water potentials at which embolism occurs in the plant. Other coordinated plant traits are then treated as sampled variables (Supporting Information: Methods S1). Water availability varies along an axis of soil water potentials. For a given combination of values of the independent plant physiological traits, the sampling procedure produces an ensemble of other trait parameter run through the model, from which the mean outcomes are then calculated. Outcomes are measured in terms of conductance loss (both stem conductance and composite conductance). Greater conductance loss indicates increasing damage to the plant. [Color figure can be viewed at wileyonlinelibrary.com]

2.3 Testing the impacts of segmentation

Given the model, a framework to characterise segmentation, and a parameterisation procedure, the effects of hydraulic and vulnerability segmentation on a plant with a given mean P_{50} , can be examined at different soil water potentials. We use conductance at a given soil water potential, expressed as a percent of maximum conductance, as a metric of plant function.

Conductance losses arise at the composite stem-leaf (k_{comp}) and stem levels (k_{stem}) . At the composite level, reductions in conductance impact transpiration and carbon fixation. At the stem/tissue level, conductance losses reflect tissue damage sustained by the plant and the carbon cost associated with replacement/repair of damaged tissues. Thus, trait combinations preserving conductance at either the composite or tissue level under given environmental conditions are advantageous (Figure 2).

We use this framework (model, segmentation parameters and conductance impact, see Figure 2) to test the hypotheses defined in the Introduction.

2.3.1 | Model metrics

The hypotheses invite two kinds of comparison.

Hypothesis I investigates the effect of the *pattern* of vulnerability segmentation. While the absence of vulnerability segmentation also represents a pattern of interest, it is useful to first consider the comparison of endpoints (reverse and conventional). The broader spectrum of vulnerability segmentation, including unsegmented plants, is further explored in Hypothesis II. Thus, the relevant test metric for Hypothesis I is the difference in conductance at a given soil water potential between plants with conventional (subscript $\it c$) and

Plant, Cell & PC Environment & PC WILEY 273

reverse vulnerability segmentation (subscript *r*), holding all other factors constant. We describe this difference at the composite level as:

$$\lambda_{\text{comp}} = \left(\frac{k_{\text{comp,c}}(\psi_{\text{soil}})}{k_{\text{comp,c,max}}} - \frac{k_{\text{comp,r}}(\psi_{\text{soil}})}{k_{\text{comp,r,max}}}\right) \times 100, \tag{15}$$

where ψ_{soil} is the soil water potential value at which the conductances are being compared. A similar comparison can be made in terms of differences in stem conductance:

$$\lambda_{\text{stem}} = \left(\frac{k_{\text{stem},c}(\psi_{\text{soil}})}{k_{\text{stem},c,\text{max}}} - \frac{k_{\text{stem},r}(\psi_{\text{soil}})}{k_{\text{stem},r,\text{max}}}\right) \times 100.$$
 (16)

Hypothesis I can be assessed by investigating the behaviour of λ_{comp} and λ_{stem} (%) for fixed values of $f_{\text{stem},0}$, mean P_{50} , ψ_{soil} , and ΔP_{50} . Positive λ values indicate greater conductance remains with conventional vulnerability segmentation, and negative values indicate a greater conductance remaining with reverse vulnerability segmentation.

Hypothesis II investigates the effect of the magnitude and directionality of vulnerability segmentation. Here, it is relevant to consider a plant with no vulnerability or hydraulic segmentation as a 'null' case. In this plant, the leaf and stem P_{50} are equivalent to the mean P_{50} , and the stem and leaves contribute equally to plant resistance. For this plant, at soil water potentials of mean P_{50} , the remaining conductance in the stem and the stem-leaf pathway as a whole will also be 50%, assuming negligible transpiration and water potential gradients within the plant. Deviations in stem and composite water potential and conductance from the null case thus measure the magnitude and direction of segmentation's effects. At the composite level, we define β as the difference between the soil water potential at which the composite conductance is equal to 50% $(\psi_{50l,k,comp=50})$ and the idealised $P_{50,mean}$:

$$\beta = P_{50,\text{mean}} - \psi_{\text{soil},k,\text{comp}=50}.$$
 (17)

Positive β (MPa) values indicate 50% loss of conductance at a soil water potential that is more negative than the mean P_{50} , and negative values indicate loss of conductance at less negative (less dry) water potentials. The more positive β is, the greater the 'benefit' of segmentation relative to the null case. It should be noted, however, that the hypothetical null case used as reference for the β value does not necessarily represent the actual performance of an unsegmented plant, as it does not consider potential water gradients within the plant. The actual performance of an unsegmented plant is modelled (case of ΔP_{50} = 0 and f_{stem} = 0.5) and its β is not necessarily equal to 0.

A similar approach can be applied to stem conductance. In the null case, 50% stem conductance remains when the soil water potential is equal to the mean P_{50} . We measure how close the segmented stem is to this state with η :

$$\eta = \frac{k_{\text{stem}}(\psi_{\text{soil},P50\text{mean}}) \times 100}{k_{\text{stem,max}}} - 50, \tag{18}$$

where η (%) describes the difference in remaining stem conductance when ψ_{soil} is equal to the mean P_{50} for the test plant as compared to the null case (wherein remaining stem conductance would be 50%). η therefore indicates how much preservation of stem conductance is prioritised as the plant experiences embolism. Positive values of η indicate greater preservation of stem conductance relative to the null case, whereas negative values indicate less preservation of stem conductance. Similar to the interpretation of β , the actual performance of an unsegmented plant is modelled and its η is not necessarily equal to 0.

These metrics are shown graphically in Figure 3, and are derived from the mean model output for fixed $f_{\text{stem,0}}$, mean P_{50} , and ΔP_{50} parameters and the ensemble of sampled traits.

2.4 | Model experiments

Four experiments were run to test the hypotheses. The variable ranges and model set-up for the experiments are summarised in Table 2. These experiments use the statistical sampling procedure for coordinated traits, described above, to fully parameterise the model.

Experiment I: To test whether conventional vulnerability segmentation results in better preservation of conductance (Hypothesis I), this experiment compares declines in conductance with declining soil water potential for plants with conventional and reverse vulnerability segmentation. It characterises these differences using λ_{comp} and λ_{stem} over a range of soil water potentials. To explore how conductance loss might change with variation in hydraulic segmentation and safety, it finds λ_{comp} and λ_{stem} for a series of discrete combinations of mean P_{50} and $f_{\text{stem},0}$. A constant magnitude of vulnerability segmentation (ΔP_{50} I = 1 MPa) is used for all scenarios. For each combination of independent variables, 750 sets of parameters are sampled using the statistical procedure for coordinated traits.

Experiment II: This experiment also makes direct comparisons between plants with conventional and reverse vulnerability segmentation (Hypothesis I), but now exploring the importance of vulnerability segmentation as safety (mean P_{50}) and hydraulic segmentation ($f_{\text{stem},0}$) are varied. To do this, it considers how λ_{comp} and λ_{stem} vary over a two-dimensional parameter space of mean P_{50} and $f_{\text{stem,0}}$. Based on the results from Experiment I, it takes the values for λ_{stem} and λ_{comp} at soil water potentials equivalent to the mean P_{50} of the plant, typically corresponding to the largest values of λ_{stem} and λ_{comp} in Experiment I. The model is used to find λ_{stem} and λ_{comp} for discrete points across the two-dimensional parameter space of 50 values each of $f_{\text{stem},0}$ and mean P_{50} , with 50 sampled parameter sets for each combination. A Gaussian filter is used to estimate the continuous two-dimensional surface from the mean of samples at each discrete point. This is done for three different magnitudes of vulnerability segmentation ($|\Delta P_{50}|$).

13659040, 2023, 9, Downloaded from https://onlinelibrary.wiley.com/doi/10.1111/pce.14649 by UNIVERSITY OF MINNESOTA 170 WILSON LIBRARY, Wiley Online Library on [27022024]. See the Terms and Conditions (https://onlinelibrary.wiley.com/doi/10.1111/pce.14649 by UNIVERSITY OF MINNESOTA 170 WILSON LIBRARY, Wiley Online Library on [27022024]. See the Terms and Conditions (https://onlinelibrary.wiley.com/doi/10.1111/pce.14649 by UNIVERSITY OF MINNESOTA 170 WILSON LIBRARY, Wiley Online Library.wiley.com/doi/10.1111/pce.14649 by UNIVERSITY OF MINNESOTA 170 WILSON LIBRARY, Wiley Online Library.wiley.com/doi/10.1111/pce.14649 by UNIVERSITY OF MINNESOTA 170 WILSON LIBRARY, Wiley Online Library.wiley.com/doi/10.1111/pce.14649 by UNIVERSITY OF MINNESOTA 170 WILSON LIBRARY, Wiley Online Library.wiley.com/doi/10.1111/pce.14649 by UNIVERSITY OF MINNESOTA 170 WILSON LIBRARY, Wiley Online Library.wiley.com/doi/10.1111/pce.14649 by UNIVERSITY OF MINNESOTA 170 WILSON LIBRARY, Wiley Online Library.wiley.com/doi/10.1111/pce.14649 by UNIVERSITY OF MINNESOTA 170 WILSON LIBRARY, Wiley Online Library.wiley.com/doi/10.1111/pce.14649 by UNIVERSITY OF MINNESOTA 170 WILSON LIBRARY, Wiley Online Library.wiley.com/doi/10.1111/pce.14649 by UNIVERSITY OF MINNESOTA 170 WILSON LIBRARY, Wiley Online Library.wiley.com/doi/10.1111/pce.14649 by UNIVERSITY OF MINNESOTA 170 WILSON LIBRARY.Wiley Online Library.wiley.com/doi/10.1111/pce.14649 by UNIVERSITY OF MINNESOTA 170 WILSON LIBRARY.Wiley Online Library.wiley.com/doi/10.1111/pce.14649 by UNIVERSITY OF MINNESOTA 170 WILSON LIBRARY.Wiley Online Library.wiley.com/doi/10.1111/pce.14649 by UNIVERSITY OF MINNESOTA 170 WILSON LIBRARY.Wiley Online Library.wiley.com/doi/10.1111/pce.14649 by UNIVERSITY OF MINNESOTA 170 WILSON LIBRARY.Wiley Online Library.wiley.com/doi/10.1111/pce.14649 by UNIVERSITY OF MINNESOTA 170 WILSON LIBRARY.Wiley Online Library.wiley

on Wiley Online Library for rules of use; OA articles are governed by the applicable Creative Commons

Metrics of Plant Function: λ , η , and β Calculated from model output of how conductances (k) change with soil water potential (ψ_s)

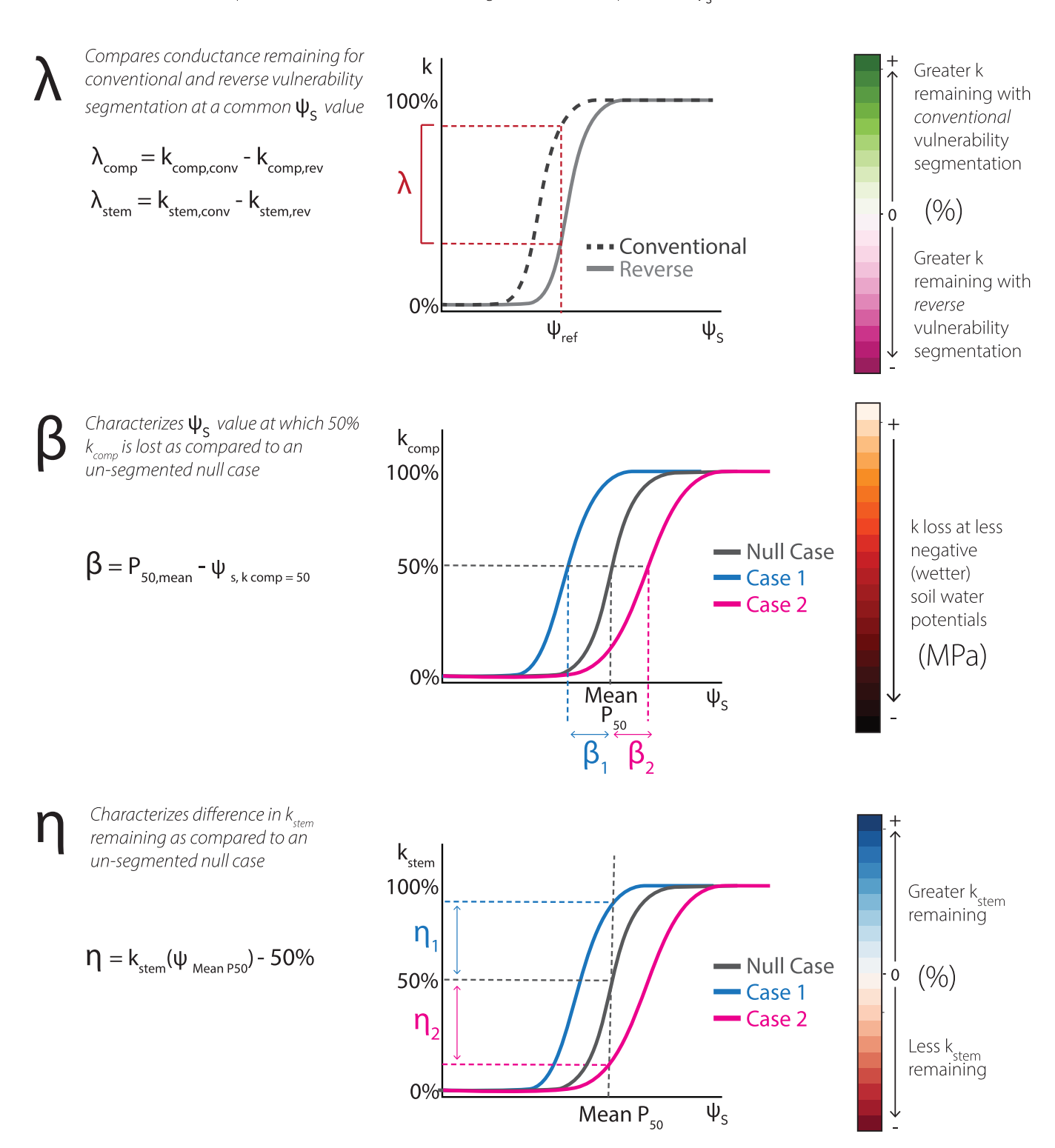


FIGURE 3 λ is used to directly compare conductance changes for plants with conventional and reverse vulnerability segmentation, but which otherwise have the same mean safety and pattern of hydraulic segmentation. To compare how variation in traits impacts plant function, the other two metrics consider how plant behaviour changes relative to the null case of a nonsegmented plant with equal mean safety (grey lines). Graphically, scenarios are shown of both a more favourable scenario (Case 1-blue line) where conductances are maintained to lower soil water potentials and a less favourable case (Case 2-pink line) where conductance is lost at less negative water potentials. Comparisons are characterised for composite conductance using β , and for stem conductance using η . Note the k values are shown as percentages of their respective maximum (unimpaired) values. [Color figure can be viewed at wileyonlinelibrary.com]

Experiment	ΔP_{50}	Mean P ₅₀	f _{stem,0}	ψ_{soil} for λ	Samples
1	11.01	-2.5, -4.5, -6.5	0.25, 0.5, 0.75	(Mean $P_{50} \pm 1.5$)	750 per combination
II	10.11, 10.51, 11.01	(-6.0, -2.0)	(0.1, 0.9)	Mean P ₅₀	50 per point (50 x 50 grid)
III	(-1.5, 1.5)	-2.0, -4.0, -6.0	(0.1, 0.9)	-	50 per point (20 x 30 grid)
IV	(-1.5, 1.5)	(-6.0, -2.0)	0.25, 0.5, 0.75	-	50 per point (20 x 30 grid)

Experiments III and IV: In the final two experiments, we consider the impacts of vulnerability segmentation and its interaction with safety and hydraulic segmentation over a range of ΔP_{50} values describing varying magnitude and direction of vulnerability segmentation (Hypothesis II). β and η are used to characterise these impacts relative to a nonsegmented base case. The interaction of vulnerability segmentation (ΔP_{50}) and hydraulic segmentation ($f_{\text{stem},0}$) is considered in Experiment III for three values of mean P_{50} . The response surface is estimated from a grid of 25 points each of ΔP_{50} and $f_{\text{stem},0}$, with 50 sampled parameter sets at each point. The interaction between vulnerability segmentation (ΔP_{50}) and safety (mean P_{50}) is considered in Experiment IV for three values of $f_{\rm stem,0}$. The response surface is estimated from a grid of 20 points of ΔP_{50} and 30 points of $f_{\text{stem.0}}$, with 50 sampled parameter sets at each point. For both experiments, the same procedure as was used in Experiment II for estimating the continuous surface is used.

2.4.1 Case study

The model is used to examine differences in function between two tree species which exhibit opposite patterns of vulnerability segmentation. Quercus douglasii (blue oak) exhibits conventional vulnerability segmentation (mean stem P₅₀ of ⁻4.29 MPa and mean leaf P₅₀ of -3.76 MPa) and Populus trichocarpa (black cottonwood) exhibits reverse vulnerability segmentation (mean stem P50 of $^{-}1.48$ MPa and mean leaf P_{50} of $^{-}2.53$ MPa). The vulnerability curves of stem and leaf xylem of Q. douglasii were measured by Skelton et al. (2019) using the optical method (Brodribb et al., 2016, 2017, 2016; Gauthey et al., 2020; Johnson et al., 2020; Skelton et al., 2017, 2018). The vulnerability curves of stem and leaf xylem of P. trichocarpa were measured in this study using the optical method. Full methodological details are presented in Methods S2. These vulnerability curves were used to parameterise the P_{50} and fitting parameters (a) of stem and leaf tissues in the model. Other parameter values were prescribed according to other literature and background data as listed in Supporting Information: Tables S2 and S3. For $f_{\text{stem.0}}$, which lacks a literature estimate, a range of values are run to create a bound around the estimates.

The composite and stem conductances are modelled for each species over a range of soil water potentials. The same analysis is then done for hypothetical cases of 'flipped' plants, wherein stem and leaf vulnerability curve parameters are interchanged (i.e., oak leaf parameters used for oak stem and vice versa) without changing any other plant variables. Changes in stem and composite conductance for the different cases are compared over a range of soil water potentials.

RESULTS

Experiment I

Experiment I considered differences between conventional and reverse vulnerability segmentation across a range of soil water potentials in terms of λ_{stem} (Figure 4) and λ_{comp} (Figure 5). For all trait combinations, λ_{stem} was positive (greater stem preservation with conventional segmentation), with the greatest values occurring when the soil water potential was approximately equivalent to the plants' mean P_{50} . λ_{stem} was greater for more negative (more safe) mean P_{50} values. The patterns were similar across the three different values of $f_{\text{stem,0}}$.

 λ_{comp} varied in sign and magnitude for the different combinations of mean P_{50} and $f_{\text{stem},0}$, indicating different advantages for vulnerability segmentation patterns. For the case of $f_{\text{stem},0} = 0.75$ (greater resistance in stems), the results were similar to those for λ_{stem} . There were positive λ_{comp} values (conventional advantage) for all mean P_{50} values, with the magnitude being greater for more negative mean P_{50} s. In contrast, for $f_{\text{stem},0}$ = 0.25 (greater resistance in leaves), λ_{comp} was generally negative (reverse advantage). The magnitude was greatest for less negative (less safe) mean P₅₀s. Further, for the most negative mean P_{50} , λ_{comp} changed from positive to negative as soil water potential declined, a switch from conventional to reverse advantage. Scenarios where $f_{\text{stem,0}} = 0.5$ were an intermediate of the two endpoints. At less negative soil water potentials, λ_{comp} was positive and then negative at more negative soil water potentials. λ_{comp} values across the range were smaller in magnitude compared to those for $f_{\text{stem,0}}$ = 0.25 and $f_{\text{stem,0}}$ = 0.75, however.

3.2 **Experiment II**

Experiment II compared conventional and reverse vulnerability segmentation with respect to changes in hydraulic segmentation $(f_{\text{stem},0})$ and safety (mean P_{50}) (instead of soil water potential as in Experiment I). For stem conductance λ_{stem} was positive across the

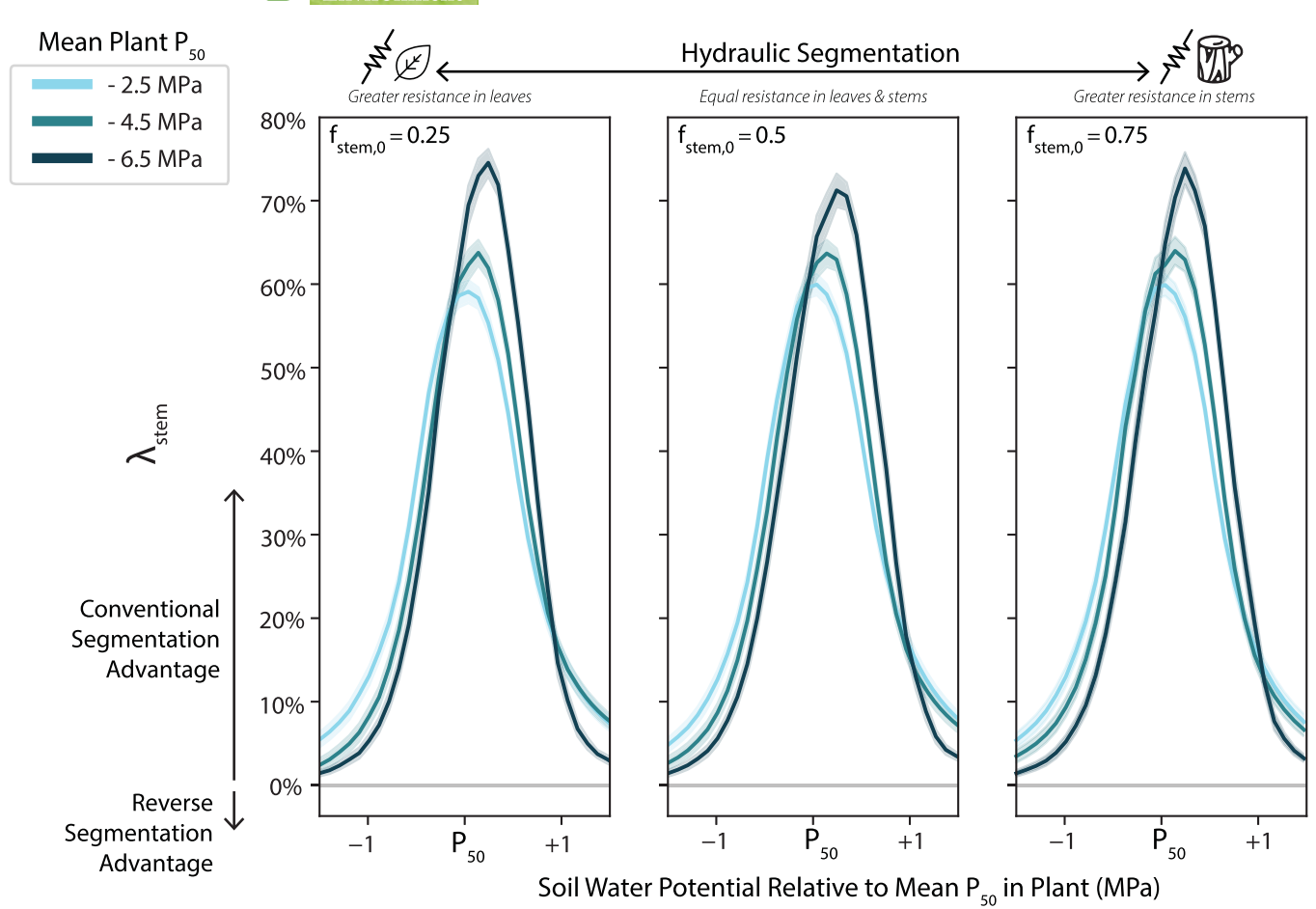


FIGURE 4 λ_{stem} over a range of soil water potential values is shown for different combinations of safety (line colours) and hydraulic segmentation (panels) in the plant with a constant $|\Delta P_{50}|$ (1.0 MPa). Soil water potentials are plotted relative to the plants mean P_{50} (ψ_{soil} - mean P_{50}). Solid lines indicate the mean value of 750 simulations and the shading indicates \pm one standard deviation. [Color figure can be viewed at wileyonlinelibrary.com]

entire parameter space, indicating that k_{stem} was best protected with conventional vulnerability segmentation (Figure 6). λ_{stem} increased with increasing vulnerability segmentation ($|\Delta P_{50}|$). For a given $|\Delta P_{50}|$, there was negligible variation in λ_{stem} with hydraulic segmentation along the *y*-axis, and a slight increase in λ_{stem} with more negative mean P_{50} values on the *x*-axis.

For composite conductance (λ_{comp}), differences between the two vulnerability segmentation patterns varied across combinations of hydraulic segmentation and safety (Figure 7). In general, higher $f_{stem,0}$ values (greater resistance in stems) yielded positive values of λ_{comp} , indicating higher composite conductance remaining with conventional vulnerability segmentation. Lower $f_{stem,0}$ values (greater resistance in leaves) yielded negative values of λ_{comp} , indicating higher composite conductance remaining with reverse vulnerability segmentation. To a lesser extent, there is also variation in λ_{comp} with the mean P_{50} value. Moving towards less negative (less safe) mean P_{50} values show a shift in λ_{comp} in the negative direction, suggesting more favourable outcomes with reverse vulnerability segmentation. Across the panels, increasing the magnitude of vulnerability segmentation

($|\Delta P_{50}|$) increased the magnitude of the differences between the vulnerability segmentation patterns.

3.3 | Experiment III

Experiment III examined how conductance loss changed with variation in hydraulic segmentation ($f_{\rm stem,0}$) and vulnerability segmentation (ΔP_{50}), across three different values of safety (mean P_{50}). η (Figure 8) shifted from positive to negative values (increasing stem damage relative to null) as ΔP_{50} went from positive (conventional segmentation) to negative (reverse segmentation). This is consistent with Experiments I and II, where greater $k_{\rm stem}$ remained with conventional segmentation. There was little change in η with changes in hydraulic segmentation along the y-axis, and the patterns and magnitudes of η values were relatively consistent for the different mean P_{50} values.

 β values were negative ($\psi_{s,kcomp=50} > P_{50,mean}$) across nearly the entire parameter space (Figure 9). Generally, there was interaction between ΔP_{50} and $f_{stem,0}$ where the least negative (most k preserving)

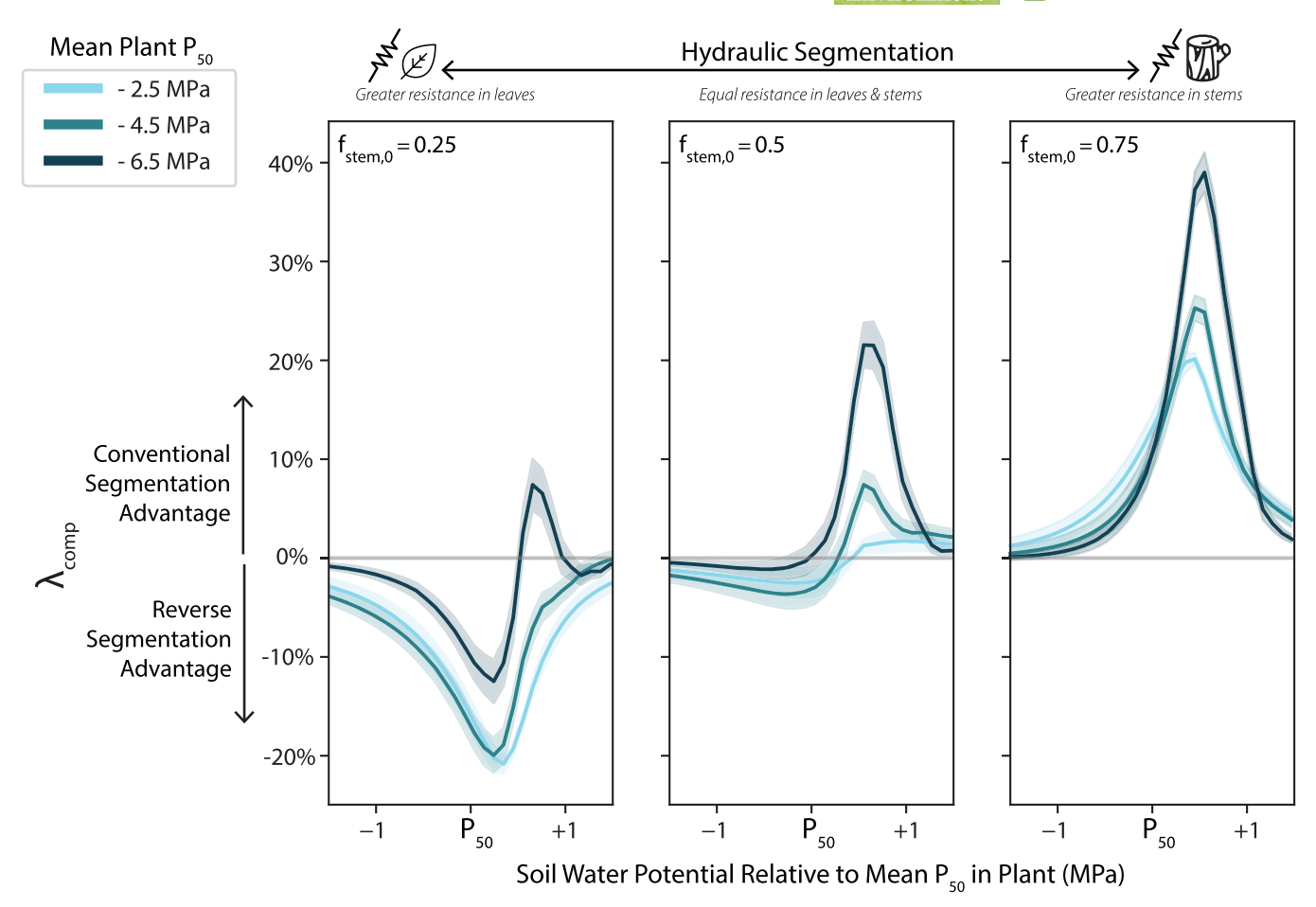


FIGURE 5 λ_{comp} over a range of soil water potential values, with the same notation and panel set-up used as in Figure 4. [Color figure can be viewed at wileyonlinelibrary.com]

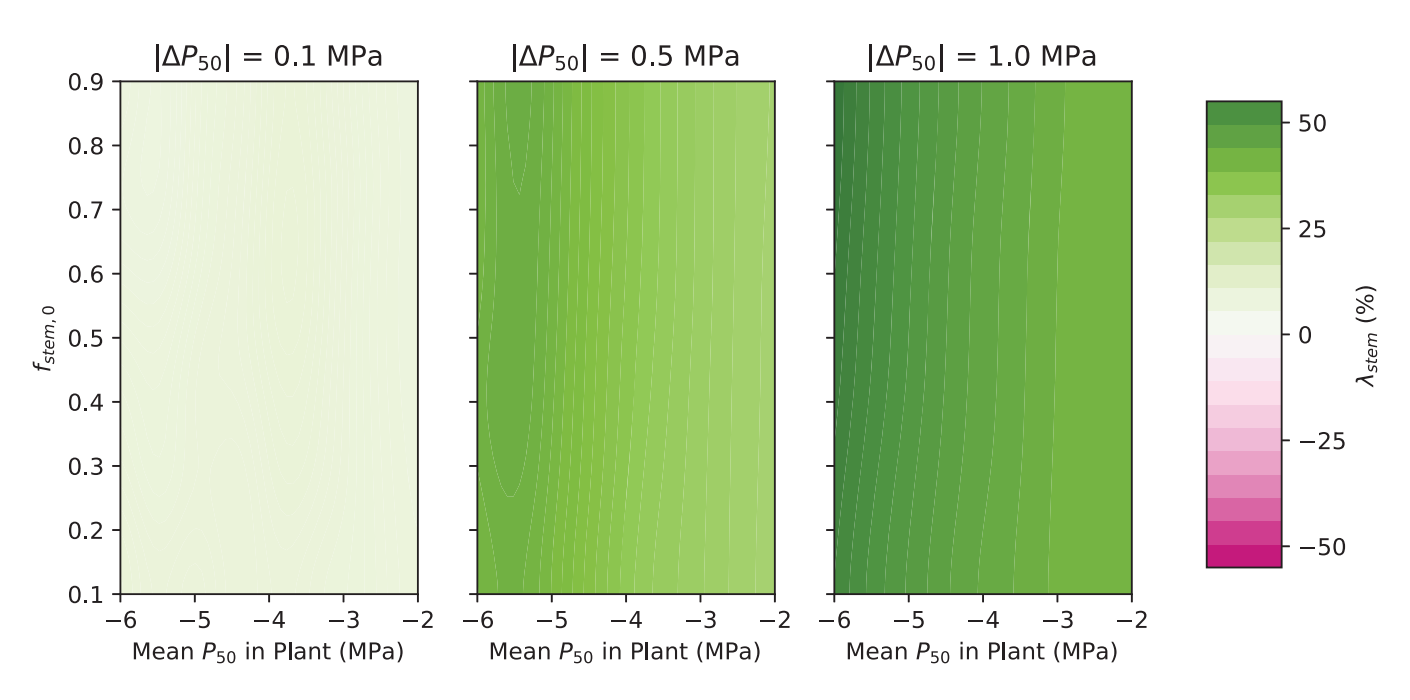


FIGURE 6 Experiment II shows λ_{stem} changes across variation in the safety (mean P_{50}) and hydraulic segmentation ($f_{\text{stem},0}$). The magnitude of vulnerability segmentation increases across the panels L to R. Green regions indicate an advantage with conventional vulnerability segmentation while advantages for reverse vulnerability segmentation are pink. [Color figure can be viewed at wileyonlinelibrary.com]

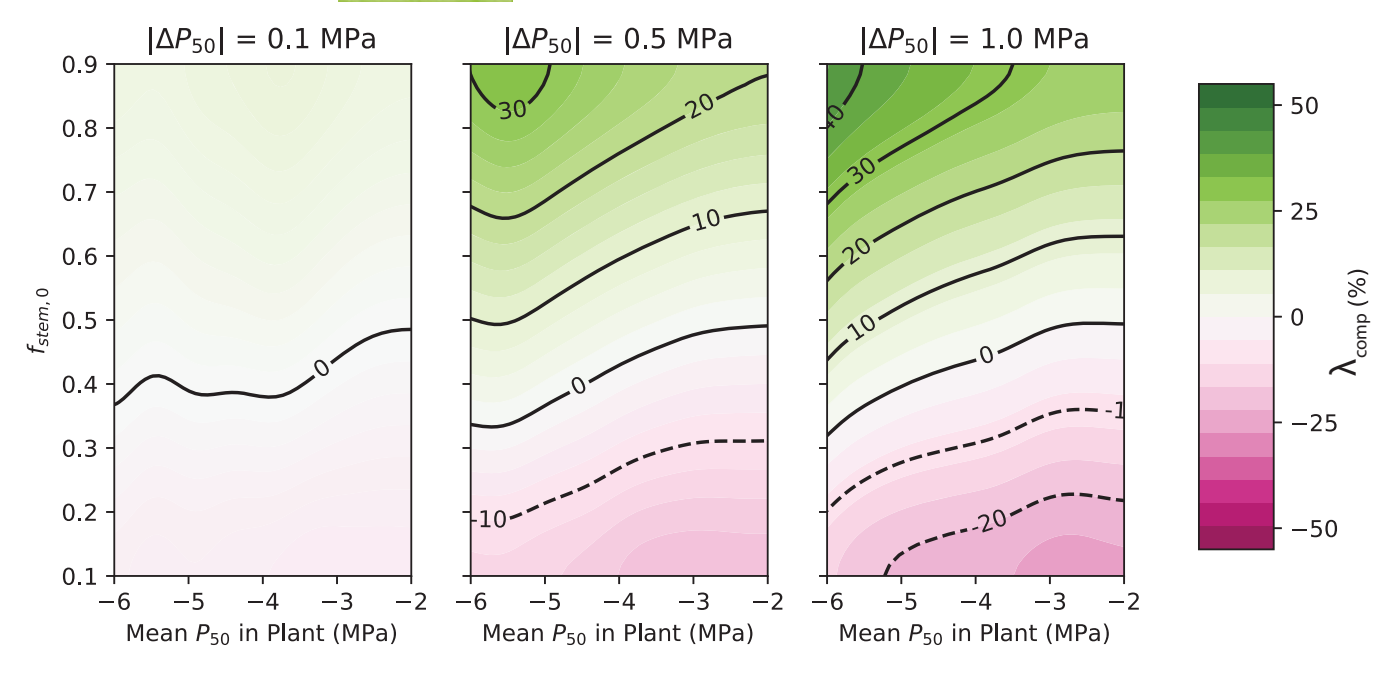


FIGURE 7 Changes in λ_{comp} for Experiment II are shown with the same set-up and notation as Figure 6. [Color figure can be viewed at wileyonlinelibrary.com]

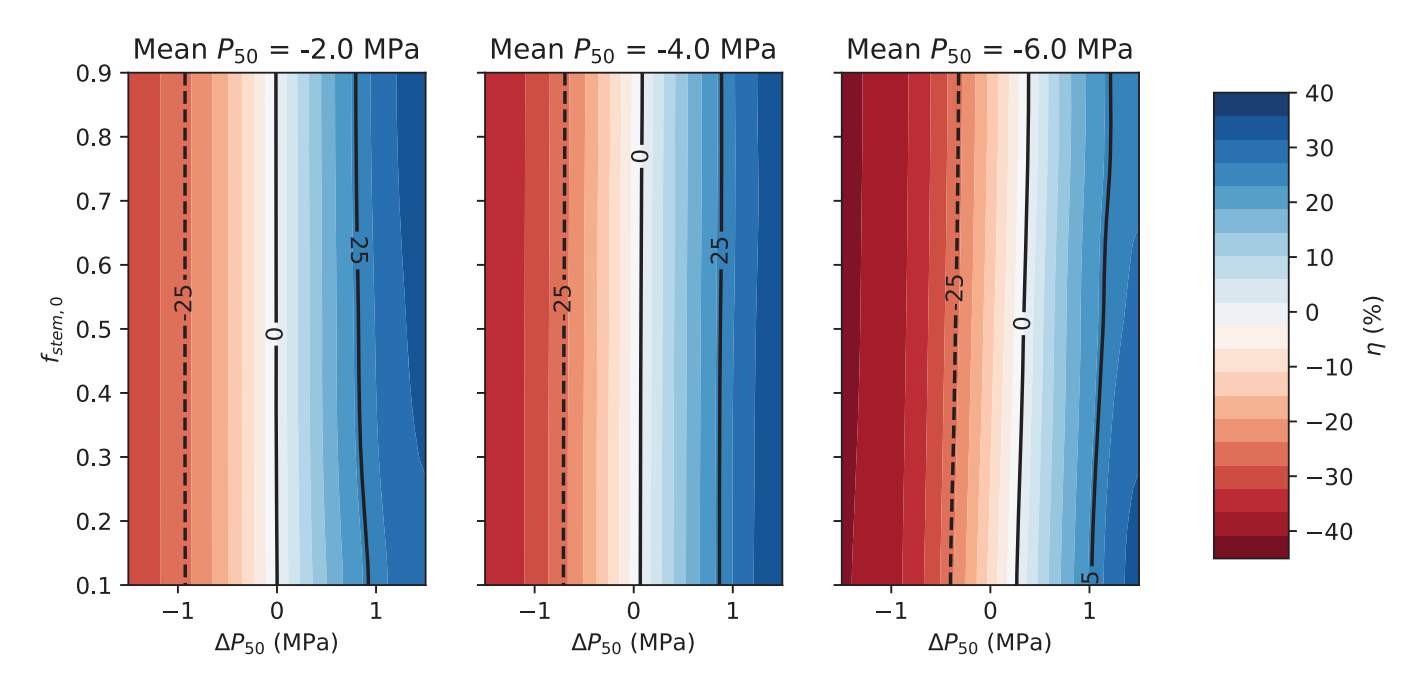


FIGURE 8 Experiment III shows η changes with variation in vulnerability segmentation (ΔP_{50}) and hydraulic segmentation ($f_{\text{stem,0}}$). The safety (mean P_{50}) increases moving from left to right across the three panels. Blue indicates higher stem conductance relative to the hypothetical null case. Red indicates lower stem conductance compared to the hypothetical null case. Contours of η values are shown with dashed and solid lines indicating negative and positive values, respectively. [Color figure can be viewed at wileyonlinelibrary.com]

 β values occurred with reverse vulnerability segmentation (negative ΔP_{50}) and greater resistance in leaves (smaller $f_{\rm stem,0}$) in combination, as well as with conventional vulnerability segmentation (positive ΔP_{50}) and greater hydraulic resistance in stems (larger $f_{\rm stem,0}$) in combination. This pattern was seen across all the safety values, with more negative (less safe) mean P_{50} values generally having slightly more negative β values across the bivariate parameter space.

3.4 | Experiment IV

In Experiment IV, the impacts on stem conductance (η) are consistent across the different patterns of hydraulic conductance (Figure 10). Positive η values (greater stem conductance remaining) are seen with positive ΔP_{50} values, with the greatest η values occurring with greater magnitudes of conventional vulnerability segmentation. Conversely,

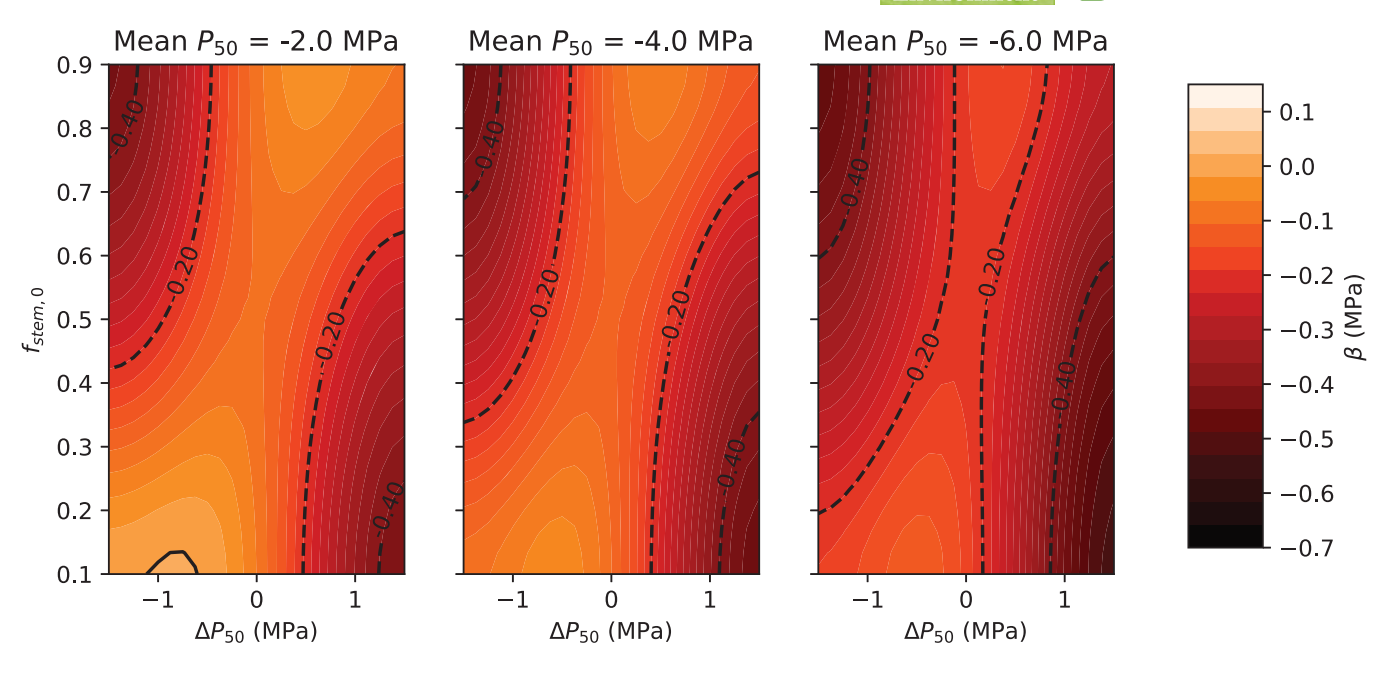


FIGURE 9 Changes in β for Experiment III are shown with the same axes and panels as Figure 8. Darker colours indicate loss of composite conductance at less negative (less dry) soil water potentials. [Color figure can be viewed at wileyonlinelibrary.com]

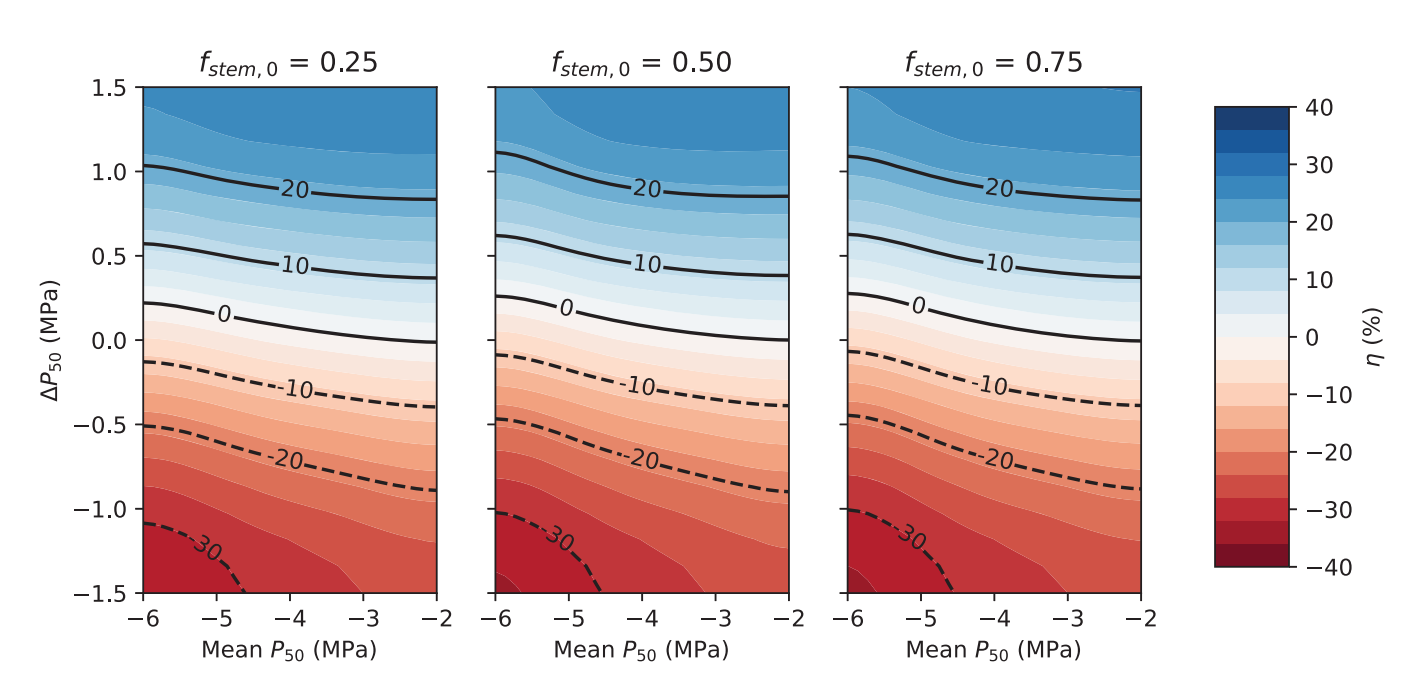


FIGURE 10 Experiment IV shows η changes with variation in safety (mean P_{50}) and vulnerability segmentation (ΔP_{50}). The proportion of resistance in the stem (f_{stem.0}) increases L to R across the panels. The colouring and contours are the same as in Figure 8. [Color figure can be viewed at wileyonlinelibrary.com]

negative η values occur with reverse vulnerability segmentation (ΔP_{50} < 0). Across constant ΔP_{50} values, there is a slight decrease in η as the mean P_{50} becomes more negative.

The interacting effects of vulnerability segmentation (ΔP_{50}) and safety (mean P_{50}) on composite conductance (Figure 11) vary with hydraulic segmentation ($f_{\text{stem,0}}$) across the three panels. Higher β values (more k preservation) occur with less negative mean P_{50} values

for a given vulnerability segmentation magnitude. However, for a given mean P₅₀ value, the effect of changing vulnerability segmentation depends on hydraulic segmentation. When hydraulic resistance is greater in leaves ($f_{\text{stem},0}$ = 0.25, left-most panel), the highest β values occur with less negative mean P_{50} values in combination with reverse vulnerability segmentation. When hydraulic resistance is instead greatest in stems ($f_{\text{stem},0} = 0.75$, right-most panel), the

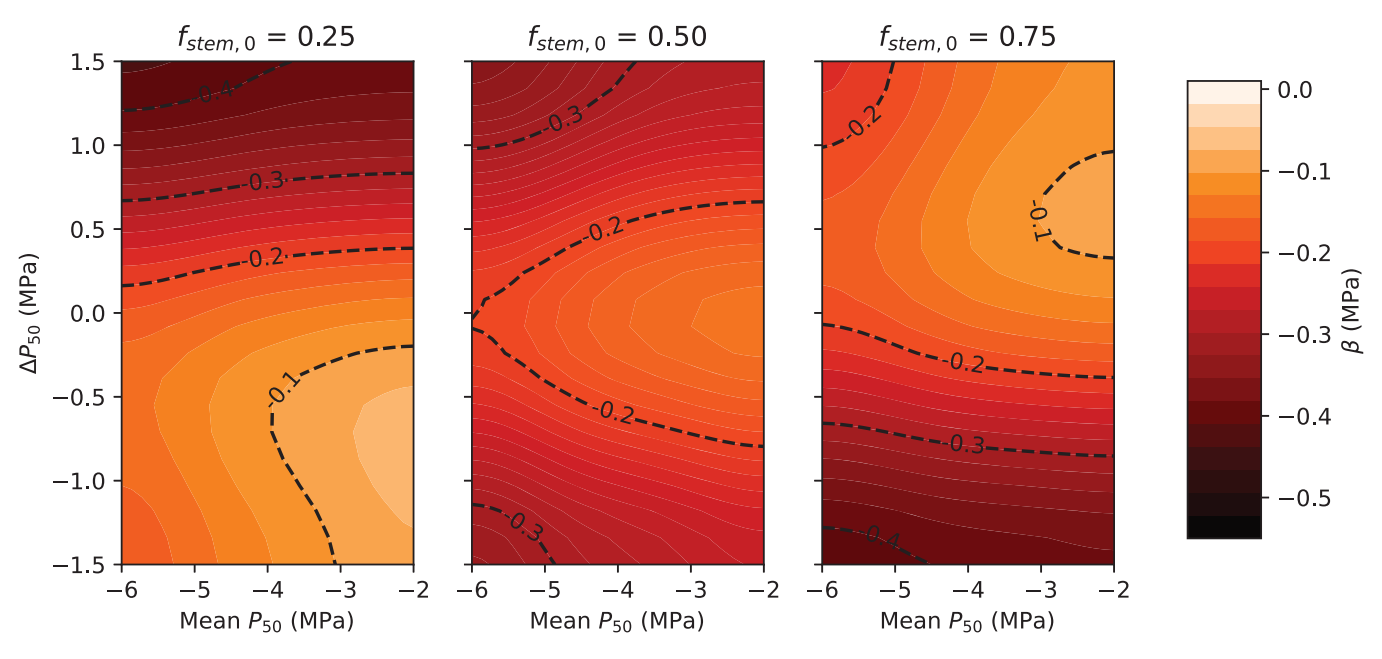


FIGURE 11 Changes in β for Experiment IV are shown with the same axes and panels as Figure 10 and the same colours and contours as Figure 9. [Color figure can be viewed at wileyonlinelibrary.com]

greatest β values occur with conventional vulnerability segmentation. For both of these endpoints, the maximum β value for a given mean P_{50} occurs when vulnerability segmentation consists of a 0.5 MPa difference between stem and leaves ($\Delta P_{50} \approx 0.5$ in the right-most panel and $\Delta P_{50} \approx -0.5$ in the left-most panel). When hydraulic resistance is equal in stems and leaves ($f_{\text{stem,0}} = 0.5$, centre panel), the greatest β values for a given mean P_{50} occur when there is no vulnerability segmentation.

3.5 | Case study

Quercus douglasii exhibits conventional vulnerability segmentation. Applying reverse segmentation to Q. douglasii caused more stem conductance loss at less negative soil water potentials for all tested $f_{stem,0}$ values (Figure 12, pink dashed lines) compared to conventional segmentation. The effect of reverse segmentation on composite conductance (blue dashed lines) varied with $f_{stem,0}$. For $f_{stem,0}$ = 0.25 (greater hydraulic resistance in leaves), loss of composite conductance occurred at more negative soil water potentials for reverse than conventional segmentation. However, for $f_{stem,0}$ = 0.75, composite conductance loss occurred at less negative soil water potential for reverse rather than conventional segmentation. For $f_{stem,0}$ = 0.5, there was no difference in loss of composite conductance between reverse and conventional segmentation.

Populus trichocarpa exhibits reverse vulnerability segmentation and was more vulnerable to embolism than Q. douglasii. Reverse and conventional vulnerability segmentation produced broadly similar conductance responses in P. trichocarpa. Conventional segmentation protected stem conductance more than reverse segmentation did for all $f_{\text{stem},0}$ values (pink dashed lines). Composite conductance losses

occurred at less negative ψ_s under conventional segmentation than reverse segmentation for $f_{\text{stem},0}$ = 0.25 (greater hydraulic resistance in leaves), at more negative ψ_s under conventional segmentation than reverse segmentation for $f_{\text{stem},0}$ = 0.75, and equivalently for both segmentation patterns for $f_{\text{stem},0}$ = 0.5.

4 | DISCUSSION

4.1 | Contrasting outcomes for preserving stem versus composite conductance

Hypothesis I posited that a plant with conventional vulnerability segmentation would experience less conductance loss than one with reverse vulnerability segmentation. Experiments I and II were consistent with this hypothesis in all cases when considering stem conductance. However, Experiments I and II also revealed scenarios, counter to Hypothesis I, in which reverse vulnerability segmentation better preserves composite conductance. Reverse vulnerability segmentation was best able to protect composite conductance when hydraulic segmentation with greater resistance in leaves occurred, and, to a lesser degree, in plants with lower safety. Conventional vulnerability segmentation does not always preserve composite conductance better than reverse vulnerability segmentation. The relative performance of the vulnerability segmentation patterns is influenced by hydraulic segmentation and safety.

Hypothesis II considered the importance of the magnitude of the vulnerability segmentation. It posited that greater magnitudes of vulnerability segmentation would produce greater differences in conductance loss relative to a nonsegmented plant. Experiments III and IV were consistent with this hypothesis for stem conductance.

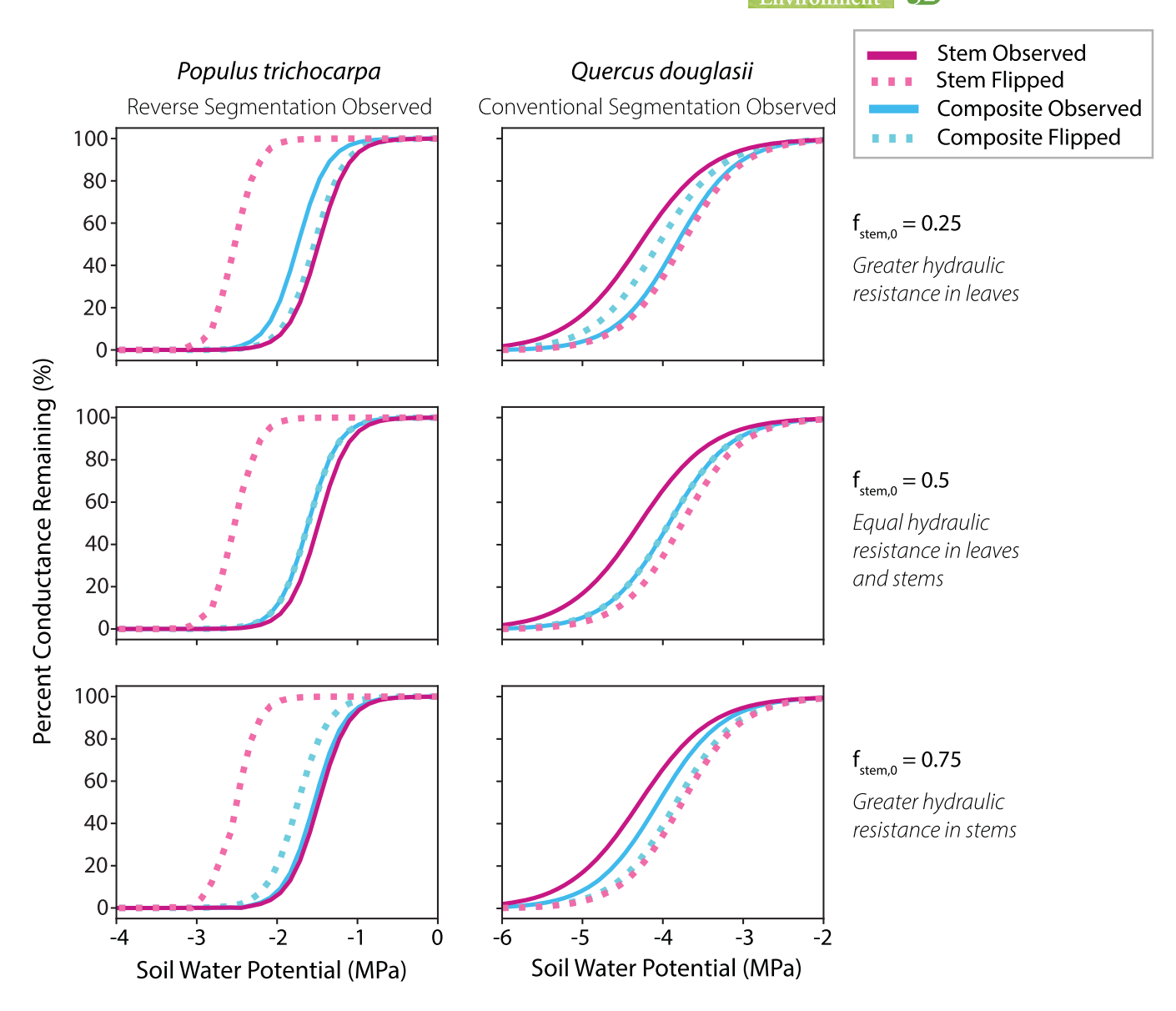


FIGURE 12 The modelled relationships between soil water potential and the stem (pink) and total (blue) conductances are shown for *Populus trichocarpa* (left column) and *Quercus douglasii* (right column). Three different values of $f_{\text{stem,0}}$ are shown across the rows. The observed vulnerability segmentation pattern is shown with solid lines and the 'flipped' (stem and leaf parameters switched) are shown with dotted lines. [Color figure can be viewed at wileyonlinelibrary.com]

Greater magnitudes of vulnerability segmentation better preserved stem conductance in conventional vulnerability segmentation and led to greater loss of stem conductance for reverse vulnerability segmentation, independently of hydraulic segmentation and safety. However, counter to Hypothesis II, Experiments III and IV revealed a nonmonotonic relationship between the magnitude of vulnerability segmentation and the preservation of composite conductance, for fixed safety and hydraulic segmentation patterns. For example, for a plant with greater hydraulic resistance in leaves, increasing the magnitude of reverse vulnerability segmentation initially leads to composite conductance loss at more negative soil water potentials than the null case. But beyond an 'optimum' vulnerability segmentation magnitude, increasing segmentation further leads to composite conductance loss at *less* negative water potentials. The 'optimum'

magnitude of vulnerability segmentation varied with hydraulic segmentation and safety.

The results showed a consistent distinction between how vulnerability segmentation impacts stem conductance and how it impacts composite conductance. The impacts of the direction and magnitude of vulnerability segmentation on composite conductance depended strongly on hydraulic segmentation, and, to a lesser degree, safety. Figure 13 summarises the interaction of hydraulic segmentation and vulnerability segmentation. These interactions were revealed in the case study, where conventional vulnerability segmentation always caused stem conductance loss to occur at more negative water potentials than reverse segmentation. For composite conductance, the effects of the vulnerability segmentation pattern depended on the hydraulic segmentation pattern. While the original

13653040, 2023, 9, Downloaded from https://onlinelibrary.

wiley.com/doi/10.1111/pce.14649 by UNIVERSITY OF MINNESOTA 170 WILSON LIBRARY, Wiley Online Library on [27/02/2024]. See the Terms,

and Conditions (https://onlinelibrary

on Wiley Online Library

for rules of use; OA articles are governed by the applicable Creative Commons

FIGURE 13 Hydraulic segmentation (y-axis) and vulnerability segmentation (x-axis) interacted to influence the relative preservation (blue, +) or loss (red, -) of hydraulic conductance at the stem tissue (k_{stem}) and composite stem-leaf (k_{comp}) levels. Evidence suggests higher resistance in leaves is more likely, constraining behaviour to the bottom two quadrants, such that variation in vulnerability segmentation can support *either* preservation of composite conductance through reverse vulnerability segmentation, *or* preservation of stem conductance through conventional vulnerability segmentation. [Color figure can be viewed at wileyonlinelibrary.com]

formulation of the Vulnerability Segmentation Hypothesis focused on stem conductance as a mechanism distinct from hydraulic segmentation, these results demonstrate the impact of vulnerability segmentation on composite conductance and its interactions with hydraulic segmentation.

4.2 | Impacts of hydraulic versus vulnerability segmentation

Zimmermann's original theory (Zimmermann, 1983) proposed that hydraulic segmentation would preserve stem conductance, yet the model experiments showed that stem conductance was much more sensitive to vulnerability segmentation than hydraulic segmentation. When plants near water potentials causing embolism, flow rates are typically suppressed by stomatal closure (Kerstiens, 1996). Differences in hydraulic resistance between tissues may not be sufficient to create large gradients in water potentials and differential embolism formation between tissues under these conditions (Tyree et al., 1993).

Hydraulic segmentation played an important role, however, in mediating the impacts of vulnerability segmentation on composite conductance. If the tissue with greater initial hydraulic resistance (lower conductance) was less vulnerable, composite conductance was better preserved compared to the opposite scenario. This interaction can be understood by considering two resistors in series. Losing 10% of conductance in the resistor with a higher initial conductance has less impact on the total conductance than a 10% loss in the less conductive

resistor. However, the experiments considered a range of hydraulic segmentation with the possibility of greater resistance in both stems and leaves, and plants traits might not traverse that entire space. Hydraulic segmentation is not well-characterised in general, but the literature that exists suggests scenarios of equal or greater resistance in leaves relative to stems ($f_{\text{stem},0} \leq 0.5$) is reasonable (Brodribb et al., 2002; Nardini & Salleo, 2000; Sack & Holbrook, 2006; Sperry et al., 1998; Yang & Tyree, 1994; Zimmermann, 1983). The model outcomes, presented in Figure 13, might, in practice, be limited to quadrants III and IV, where promoting preservation of *either* stem or composite conductance is possible depending on the vulnerability segmentation pattern, but not both. Further work to characterise hydraulic segmentation and vulnerability segmentation in tandem is needed.

The experiments also showed that safety modulates the effects of segmentation pattern on plants. This could be due to covariation with other traits enforced through the parameterisation process (Gleason et al., 2016). Coordination between vulnerability segmentation and other traits was not considered in this study (due to lack of data), and also represents a potentially important avenue for study.

4.3 | Implications for understanding of whole-plant plant hydraulics and plant drought response

The model results reiterate findings that the impact of plant physiology on plant function is not strictly a result of individual traits, but emerges from the suite of traits in a plant. A more holistic approach to physiological traits and their impact on function could explain the diversity and variation in traits observed across and within environments. Simple modelling approaches, such as the one developed in this study, are helpful in approaching such a holistic paradigm, by revealing the interactions of multiple traits and environmental conditions on plant function (Feng et al., 2019, 2018, 2017; Kannenberg et al., 2022; Trugman, 2022).

These model experiments demonstrated that conventional vulnerability segmentation does indeed support the preservation of stem conductance under declining water potentials, thereby better protecting carbon that has already been assimilated and stored within the plant. However, the results also demonstrated a potential reason why conventional vulnerability has not been observed to be ubiquitous. The experiments revealed scenarios where reverse vulnerability segmentation better supports the preservation of composite conductance. Preservation of composite conductance, even at a cost of stem conductance, could reflect specific plant drought response strategies that prioritise maintenance of carbon uptake during drought. As such, these results suggest a functional implication across the spectrum of vulnerability segmentation patterns from those that prioritise composite conductance and continued carbon uptake (reverse) to those that prioritise stem conductance and invested carbon (conventional), with unsegmented plants representing an intermediate compromise between the endpoints. The degree of these functional implications are then shown to

-WILEY

be further modulated by the pattern of hydraulic segmentation within the plant. These considerations add a temporal dimension to the tradeoffs between water and carbon under drought conditions, with implications for fluxes and mortality which remain difficult to describe within current hydraulic frameworks (Anderegg et al., 2016; De Kauwe et al., 2020; Powers et al., 2020; Rowland et al., 2021; Trugman, 2022; Trugman et al., 2021; Venturas et al., 2021).

The favorability of drought response strategies is itself complex and dependent on climatic, edaphic and topographic conditions (McLaughlin et al., 2020). However, it is notable that the case study species, with opposite segmentation strategies, overlap in their ranges in California (Supporting Information: Figure S3), but are found in different locations in the landscape. P. trichocarpa is a riparian species, while Q. douglasii is usually found on drier sites within the landscape. Thus, even for similar climatic conditions, these species would likely have different experiences of water deficit (Ackerly et al., 2020; Dawson et al., 2020; McLaughlin et al., 2017, 2020; Tai et al., 2017). The observations of vulnerability segmentation, and reverse segmentation in particular, are still fairly limited, making it difficult to ascertain what broader patterns may exist. However, there are some similarities with previous studies. Levionnois et al. (2020) and Villagra et al. (2013) both observed reverse vulnerability in neotropical species, which would not be expected to experience prolonged and severe water deficits. Similarly, Skelton et al. (2018) found that Q. sadleriana, typically found in moist understory environments in Pacific Northwest temperate rainforests, exhibited earlier onset of cavitation in stems than leaves and was also the most vulnerable of the measured oak species in the Western United States. Further studies have the potential to better understand potential links between vulnerability segmentation pattern and physical environmental conditions. Modelling studies that consider how potential strategies perform in terms of carbon fixation and hydraulic damage under dynamic hydrological conditions (including water deficits of varying severity, duration and frequency) could help to reveal when certain strategies may be favourable.

It is important to note that plants mediate their drought response by many additional mechanisms (Pivovaroff et al., 2016). Particularly, it could be important to consider how else leaves can act as 'fuses' to protect stems, such as through stomatal regulation (Buckley, 2019), minimum leaf conductance (Duursma et al., 2019), or drought deciduousness (Wolfe et al., 2016). Beyond the hydraulic differences between stem and leaf xylem that were the focus of this study, hydraulic properties can also vary within tissue types (Couvreur et al., 2018; Grönlund et al., 2016), and outside-xylem pathways can contribute to leaf hydraulic decline (Scoffoni, Albuquerque, et al., 2017; Scoffoni, Sack, et al., 2017). This study did not consider how roots can also act as a hydraulic 'fuse', although roots can also have distinct vulnerability from stem and leaf tissues (Creek et al., 2018; Peters et al., 2020; Wu et al., 2020). Additionally, it could be important to consider how plant capacitance plays a dynamic role in mediating plant water potentials and drought response (McCulloh et al., 2019), and further work to

consider how this might be coordinated with vulnerability segmentation is warranted. These mechanisms will add complexity to the ways in which vulnerability segmentation impacts plant function and fluxes.

ACKNOWLEDGEMENTS

We would like to thank Jessica Diaz for assistance with the vulnerability measurements for Populus trichocarpa. This work was supported by a National Science Foundation Graduate Research Fellowship (Grant No. DGE 1752814 to Jean V. Wilkening); a National Science Foundation CAREER Award (Grant No. DEB-2045610 to Xue Feng); and a FLAIR Fellowship from the British Royal Society and the African Academy of Sciences (Award No. FLR\R1\191609 to Robert P. Skelton). The FLAIR Fellowship Programme is a partnership between the African Academy of Sciences and the Royal Society funded by the UK Government's Global Challenges Research Fund.

DATA AVAILABILITY STATEMENT

The model code is available at https://github.com/jvwilkening/ Segmentation_Hydraulic_Model.

ORCID

Jean V. Wilkening https://orcid.org/0000-0002-9229-6464 Robert P. Skelton https://orcid.org/0000-0003-2768-6420 Xue Feng http://orcid.org/0000-0003-1381-3118 Todd E. Dawson https://orcid.org/0000-0002-6871-3440 Sally E. Thompson https://orcid.org/0000-0003-4618-5066

REFERENCES

Ackerly, D.D., Kling, M.M., Clark, M.L., Papper, P., Oldfather, M.F., Flint, A.L. & Flint, L.E. (2020) Topoclimates, refugia, and biotic responses to climate change. Frontiers in Ecology and the Environment, 18(5), 288-297.

Anderegg, W.R., Klein, T., Bartlett, M., Sack, L., Pellegrini, A.F. A., Choat, B. & Jansen, S. (2016) Meta-analysis reveals that hydraulic traits explain cross-species patterns of drought-induced tree mortality across the globe. Proceedings of the National Academy of Sciences United States of America, 113(18), 5024-5029. https://doi.org/10. 1073/pnas.1525678113

Bartlett, M.K., Klein, T., Jansen, S., Choat, B. & Sack, L. (2016) The correlations and sequence of plant stomatal, hydraulic, and wilting responses to drought. Proceedings of the National Academy of Sciences United States of America, 113(46), 13098-13103.

Blackman, C.J., Li, X., Choat, B., Rymer, P.D., De Kauwe, M.G., Duursma, R.A., Tissue, D.T. & Medlyn, B.E. (2019) Desiccation time during drought is highly predictable across species of eucalyptus from contrasting climates. New Phytologist, 224(2), 632-643.

Bonan, G.B. (2008) Forests and climate change: forcings, feedbacks, and the climate benefits of forests. Science, 320(5882), 1444-1449.

Bouche, P.S., Delzon, S., Choat, B., Badel, E., Brodribb, T.J., Burlett, R., Cochard, H., Charra-Vaskou, K., Lavigne, B., Li, S. et al. (2016) Are needles of Pinus pinaster more vulnerable to xylem embolism than branches? new insights from X-ray computed tomography. Plant, Cell & Environment, 39(4), 860-870.

Brodribb, T., Holbrook, N.M. & Gutierrez, M. (2002) Hydraulic and photosynthetic co-ordination in seasonally dry tropical forest trees. Plant, Cell & Environment, 25(11), 1435-1444.

- Brodribb, T.J., Bienaimé, D. & Marmottant, P. (2016) Revealing catastrophic failure of leaf networks under stress. Proceedings of the National Academy of Sciences United States of America, 113(17), 4865-4869.
- Brodribb, T.J., Carriqui, M., Delzon, S. & Lucani, C. (2017) Optical measurement of stem xylem vulnerability. Plant Physiology, 174(4), 2054-2061.
- Brodribb, T.J., Skelton, R.P., McAdam, S.A., Bienaimé, D., Lucani, C.J. & Marmottant, P. (2016) Visual quantification of embolism reveals leaf vulnerability to hydraulic failure. New Phytologist, 209(4), 1403-1409.
- Bucci, S.J., Scholz, F.G., Campanello, P.I., Montti, L., Jimenez-Castillo, M., Rockwell, F.A., Manna, L.L., Guerra, P., Bernal, P.L., Troncoso, O. et al. (2012) Hydraulic differences along the water transport system of south American nothofagus species: do leaves protect the stem functionality? Tree Physiology, 32(7), 880-893.
- Buckley, T.N. (2019) How do stomata respond to water status? New Phytologist, 224(1), 21-36.
- Charra-Vaskou, K., Badel, E., Burlett, R., Cochard, H., Delzon, S. & Mayr, S. (2012) Hydraulic efficiency and safety of vascular and non-vascular components in Pinus pinaster leaves. Tree Physiology, 32(9), 1161-1170.
- Charrier, G., Delzon, S., Domec, J.-C., Zhang, L., Delmas, C.E., Merlin, I., Corso, D., King, A., Ojeda, H., Ollat, N. et al. (2018) Drought will not leave your glass empty: low risk of hydraulic failure revealed by longterm drought observations in world's top wine regions. Science Advances, 4(1), eaao6969.
- Charrier, G., Torres-Ruiz, J.M., Badel, E., Burlett, R., Choat, B., Cochard, H., Delmas, C.E., Domec, J.-C., Jansen, S., King, A. et al. (2016) Evidence for hydraulic vulnerability segmentation and lack of xylem refilling under tension. Plant Physiology, 172(3), 1657-1668.
- Chen, J.-W., Zhang, Q., Li, X.-S. & Cao, K.-F. (2009) Independence of stem and leaf hydraulic traits in six Euphorbiaceae tree species with contrasting leaf phenology. Planta, 230(3), 459-468.
- Choat, B., Ball, M.C., Luly, J.G. & Holtum, J.A. (2005) Hydraulic architecture of deciduous and evergreen dry rainforest tree species from north-eastern Australia. Trees, 19(3), 305-311.
- Choat, B., Brodribb, T.J., Brodersen, C.R., Duursma, R.A., López, R. & Medlyn, B.E. (2018) Triggers of tree mortality under drought. Nature, 558(7711), 531-539,
- Cochard, H., Bréda, N., Granier, A. & Aussenac, G. (1992) Vulnerability to air embolism of three European oak species (Quercus petraea (matt) liebl, q pubescens willd, q robur l). Annales des Sciences Forestières, 49, 225-233.
- Cochard, H. & Delzon, S. (2013) Hydraulic failure and repair are not routine in trees. Annals of Forest Science, 70(7), 659-661.
- Cochard, H., Delzon, S. & Badel, E. (2015) X-ray microtomography (micro-CT): a reference technology for high-resolution quantification of xylem embolism in trees. Plant, Cell & Environment, 38(1), 201-206.
- Cochard, H., Lemoine, D. & Dreyer, E. (1999) The effects of acclimation to sunlight on the xylem vulnerability to embolism in Fagus sylvatica I. Plant, Cell & Environment, 22(1), 101-108.
- Couvreur, V., Ledder, G., Manzoni, S., Way, D.A., Muller, E.B. & Russo, S.E. (2018) Water transport through tall trees: a vertically explicit, analytical model of xylem hydraulic conductance in stems. Plant, Cell & Environment, 41(8), 1821-1839.
- Creek, D., Blackman, C.J., Brodribb, T.J., Choat, B. & Tissue, D.T. (2018) Coordination between leaf, stem, and root hydraulics and gas exchange in three arid-zone angiosperms during severe drought and recovery. Plant, Cell & Environment, 41(12), 2869-2881.
- Davis, S.D., Sperry, J.S. & Hacke, U.G. (1999) The relationship between xylem conduit diameter and cavitation caused by freezing. American Journal of Botany, 86(10), 1367-1372.
- Dawson, T.E., Hahm, W.J. & Crutchfield-Peters, K. (2020) Digging deeper: what the critical zone perspective adds to the study of plant ecophysiology. New Phytologist, 226(3), 666-671.
- De Kauwe, M. G., Medlyn, B.E., Ukkola, A.M., Mu, M., Sabot, M.E., Pitman, A.J., Meir, P., Cernusak, L.A., Rifai, S.W., Choat, B. et al.

- (2020) Identifying areas at risk of drought-induced tree mortality across south-eastern Australia. Global Change Biology, 26(10), 5716-5733.
- Dixon, H.H. & Joly, J. (1894) On the ascent of sap. Proceedings of the Royal Society of London, 57, 3-5.
- Duursma, R.A., Blackman, C.J., Lopéz, R., Martin-StPaul, N.K., Cochard, H. & Medlyn, B.E. (2019) On the minimum leaf conductance: its role in models of plant water use, and ecological and environmental controls. New Phytologist, 221(2), 693-705.
- Eller, C.B., de V., Barros, F., Bittencourt, P.R., Rowland, L., Mencuccini, M. & Oliveira, R.S. (2018) Xylem hydraulic safety and construction costs determine tropical tree growth. Plant, Cell & Environment, 41(3),
- Feng, X., Ackerly, D.D., Dawson, T.E., Manzoni, S., McLaughlin, B., Skelton, R.P., Vico, G., Weitz, A.P. & Thompson, S.E. (2019) Beyond isohydricity: the role of environmental variability in determining plant drought responses. Plant, Cell & Environment, 42(4), 1104-1111.
- Feng, X., Ackerly, D.D., Dawson, T.E., Manzoni, S., Skelton, R.P., Vico, G. & Thompson, S.E. (2018) The ecohydrological context of drought and classification of plant responses. Ecology Letters, 21(11), 1723-1736,
- Feng, X., Dawson, T.E., Ackerly, D.D., Santiago, L.S. & Thompson, S.E. (2017) Reconciling seasonal hydraulic risk and plant water use through probabilistic soil-plant dynamics. Global Change Biology, 23(9), 3758-3769,
- Gauthey, A., Peters, J.M., Carins-Murphy, M.R., Rodriguez-Dominguez, C.M., Li, X., Delzon, S., King, A., López, R., Medlyn, B.E., Tissue, D.T. et al. (2020) Visual and hydraulic techniques produce similar estimates of cavitation resistance in woody species. New Phytologist, 228(3), 884-897.
- Gleason, S.M., Westoby, M., Jansen, S., Choat, B., Hacke, U.G., Pratt, R.B., Bhaskar, R., Brodribb, T.J., Bucci, S.J., Cao, K.-F. et al. (2016) Weak tradeoff between xylem safety and xylem-specific hydraulic efficiency across the world's woody plant species. New Phytologist, 209(1), 123-136
- Grönlund, L., Hölttä, T. & Mäkelä, A. (2016) Branch age and light conditions determine leaf-area-specific conductivity in current shoots of Scots pine. Tree Physiology, 36(8), 994-1006.
- Guan, X., Werner, J., Cao, K.-F., Pereira, L., Kaack, L., McAdam, S. & Jansen, S. (2022) Stem and leaf xylem of angiosperm trees experiences minimal embolism in temperate forests during two consecutive summers with moderate drought. Plant Biology, 24(7), 1208-1223.
- Hacke, U.G., Sperry, J.S. & Pittermann, J. (2005) Efficiency versus safety tradeoffs for water conduction in angiosperm vessels versus gymnosperm tracheids. Vascular Transport in Plants, 333-353.
- Hao, G.-Y., Hoffmann, W.A., Scholz, F.G., Bucci, S.J., Meinzer, F.C., Franco, A.C., Cao, K.-F. & Goldstein, G. (2008) Stem and leaf hydraulics of congeneric tree species from adjacent tropical savanna and forest ecosystems. Oecologia, 155(3), 405-415.
- Hargrave, K., Kolb, K., Ewers, F. & Davis, S. (1994) Conduit diameter and drought-induced embolism in Salvia mellifera greene (Labiatae). New Phytologist, 126(4), 695-705.
- Hochberg, U., Albuquerque, C., Rachmilevitch, S., Cochard, H., David-Schwartz, R., Brodersen, C.R., McElrone, A. & Windt, C.W. (2016) Grapevine petioles are more sensitive to drought induced embolism than stems: evidence from in vivo MRI and microcomputed tomography observations of hydraulic vulnerability segmentation. Plant, Cell & Environment, 39(9), 1886-1894.
- Hochberg, U., Windt, C.W., Ponomarenko, A., Zhang, Y.-J., Gersony, J., Rockwell, F.E. & Holbrook, N.M. (2017) Stomatal closure, basal leaf embolism, and shedding protect the hydraulic integrity of grape stems. Plant Physiology, 174(2), 764-775.
- Holbrook, N.M., Ahrens, E.T., Burns, M.J. & Zwieniecki, M.A. (2001) In vivo observation of cavitation and embolism repair using magnetic resonance imaging. Plant Physiology, 126(1), 27-31.



- Johnson, D., McCulloh, K., Meinzer, F., Woodruff, D. & Eissenstat, D. (2011) Hydraulic patterns and safety margins, from stem to stomata, in three eastern US tree species. Tree Physiology, 31(6), 659–668.
- Johnson, D.M., Wortemann, R., McCulloh, K.A., Jordan-Meille, L., Ward, E., Warren, J.M., Palmroth, S. & Domec, J.-C. (2016) A test of the hydraulic vulnerability segmentation hypothesis in angiosperm and conifer tree species. *Tree Physiology*, 36(8), 983–993.
- Johnson, K.M., Brodersen, C., Carins-Murphy, M.R., Choat, B. & Brodribb, T.J. (2020) Xylem embolism spreads by single-conduit events in three dry forest angiosperm stems. *Plant Physiology*, 184(1), 212–222.
- Kannenberg, S.A., Guo, J.S., Novick, K.A., Anderegg, W.R., Feng, X., Kennedy, D., Konings, A.G., Martínez-Vilalta, J. & Matheny, A.M. (2022) Opportunities, challenges and pitfalls in characterizing plant water-use strategies. *Functional Ecology*, 36(1), 24–37.
- Kattge, J., Bönisch, G., Díaz, S., Lavorel, S., Prentice, I.C., Leadley, P., Tautenhahn, S., Werner, G.D., Aakala, T., Abedi, M. et al. (2020) Try plant trait database-enhanced coverage and open access. *Global Change Biology*, 26(1), 119–188.
- Kerstiens, G. (1996) Cuticular water permeability and its physiological significance. *Journal of Experimental Botany*, 47(12), 1813–1832.
- Klepsch, M., Zhang, Y., Kotowska, M.M., Lamarque, L.J., Nolf, M., Schuldt, B., Torres-Ruiz, J.M., Qin, D.-W., Choat, B., Delzon, S. et al. (2018) Is xylem of angiosperm leaves less resistant to embolism than branches? insights from micro CT, hydraulics, and anatomy. *Journal of Experimental Botany*, 69(22), 5611–5623.
- Larter, M., Pfautsch, S., Domec, J.-C., Trueba, S., Nagalingum, N. & Delzon, S. (2017) Aridity drove the evolution of extreme embolism resistance and the radiation of conifer genus Callitris. New Phytologist, 215(1), 97–112.
- Levionnois, S., Kaack, L., Heuret, P., Abel, N., Ziegler, C., Coste, S., Stahl, C. & Jansen, S. (2022) Pit characters determine drought-induced embolism resistance of leaf xylem across 18 neotropical tree species. *Plant Physiology*, 190(1), 371–386.
- Levionnois, S., Ziegler, C., Heuret, P., Jansen, S., Stahl, C., Calvet, E., Goret, J.-Y., Bonal, D. & Coste, S. (2021) Is vulnerability segmentation at the leaf-stem transition a drought resistance mechanism? a theoretical test with a trait-based model for neotropical canopy tree species. *Annals of Forest Science*, 78(4), 1–16.
- Levionnois, S., Ziegler, C., Jansen, S., Calvet, E., Coste, S., Stahl, C., Salmon, C., Delzon, S., Guichard, C. & Heuret, P. (2020) Vulnerability and hydraulic segmentations at the stem-leaf transition: coordination across neotropical trees. *New Phytologist*, 228(2), 512–524.
- Li, X., Delzon, S., Torres-Ruiz, J., Badel, E., Burlett, R., Cochard, H., Jansen, S., King, A., Lamarque, L.J., Lenoir, N. et al. (2020) Lack of vulnerability segmentation in four angiosperm tree species: evidence from direct X-ray microtomography observation. *Annals of Forest Science*, 77(2), 1–12.
- Losso, A., Bär, A., Dämon, B., Dullin, C., Ganthaler, A., Petruzzellis, F., Savi, T., Tromba, G., Nardini, A., Mayr, S. et al. (2019) Insights from in vivo micro-ct analysis: testing the hydraulic vulnerability segmentation in Acer pseudoplatanus and Fagus sylvatica seedlings. New Phytologist, 221(4), 1831–1842.
- Manzoni, S., Vico, G., Katul, G., Palmroth, S. & Porporato, A. (2014) Optimal plant water-use strategies under stochastic rainfall. Water Resources Research, 50(7), 5379–5394.
- Martínez-Vilalta, J., Prat, E., Oliveras, I. & Piñol, J. (2002) Hydraulic properties of roots and stems of nine woody species from a holm oak forest in ne Spain. *Oecologia*, 133(1), 19–29.
- McCulloh, K.A., Domec, J.-C., Johnson, D.M., Smith, D.D. & Meinzer, F.C. (2019) A dynamic yet vulnerable pipeline: integration and coordination of hydraulic traits across whole plants. *Plant, Cell & Environment*, 42(10), 2789–2807.
- McDowell, N., Pockman, W.T., Allen, C.D., Breshears, D.D., Cobb, N., Kolb, T., Plaut, J., Sperry, J.S., West, A., Williams, D.G. et al. (2008)

- Mechanisms of plant survival and mortality during drought: why do some plants survive while others succumb to drought? New Phytologist, 178(4), 719–739.
- McLaughlin, B.C., Ackerly, D.D., Klos, P.Z., Natali, J., Dawson, T.E. & Thompson, S.E. (2017) Hydrologic refugia, plants, and climate change. Global Change Biology, 23(8), 2941–2961.
- McLaughlin, B.C., Blakey, R., Weitz, A.P., Feng, X., Brown, B.J., Ackerly, D.D., Dawson, T.E. & Thompson, S.E. (2020) Weather underground: subsurface hydrologic processes mediate tree vulnerability to extreme climatic drought. Global Change Biology, 26(5), 3091–3107.
- Mursinna, A.R., McCormick, E., Van Horn, K., Sartin, L. & Matheny, A.M. (2018) Plant hydraulic trait covariation: a global meta-analysis to reduce degrees of freedom in trait-based hydrologic models. Forests, 9(8), 446. https://doi.org/10.3390/f9080446
- Nardini, A. & Salleo, S. (2000) Limitation of stomatal conductance by hydraulic traits: sensing or preventing xylem cavitation? *Trees*, 15(1), 14–24.
- Nolf, M., Beikircher, B., Rosner, S., Nolf, A. & Mayr, S. (2015) Xylem cavitation resistance can be estimated based on time-dependent rate of acoustic emissions. New Phytologist, 208(2), 625–632.
- Nolf, M., Creek, D., Duursma, R., Holtum, J., Mayr, S. & Choat, B. (2015) Stem and leaf hydraulic properties are finely coordinated in three tropical rain forest tree species. *Plant, Cell & Environment*, 38(12), 2652–2661.
- Pammenter, N.v. & Van der Willigen, C. (1998) A mathematical and statistical analysis of the curves illustrating vulnerability of xylem to cavitation. *Tree Physiology*, 18(8–9), 589–593.
- Peters, J.M., Gauthey, A., Lopez, R., Carins-Murphy, M.R., Brodribb, T.J. & Choat, B. (2020) Non-invasive imaging reveals convergence in root and stem vulnerability to cavitation across five tree species. *Journal* of Experimental Botany, 71(20), 6623–6637.
- Petruzzellis, F., Tomasella, M., Miotto, A., Natale, S., Trifilò, P. & Nardini, A. (2020) A leaf selfie: using a smartphone to quantify leaf vulnerability to hydraulic dysfunction. *Plants*, 9(2), 234.
- Pittermann, J., Sperry, J.S., Wheeler, J.K., Hacke, U.G. & Sikkema, E.H. (2006) Mechanical reinforcement of tracheids compromises the hydraulic efficiency of conifer xylem. Plant, Cell & Environment, 29(8), 1618–1628.
- Pivovaroff, A.L., Pasquini, S.C., De Guzman, M.E., Alstad, K.P., Stemke, J.S. & Santiago, L.S. (2016) Multiple strategies for drought survival among woody plant species. *Functional Ecology*, 30(4), 517–526.
- Ponomarenko, A., Vincent, O., Pietriga, A., Cochard, H., Badel, É. & Marmottant, P. (2014) Ultrasonic emissions reveal individual cavitation bubbles in water-stressed wood. *Journal of the Royal Society Interface*, 11(99), 20140480.
- Powers, J.S., Vargas G, G., Brodribb, T.J., Schwartz, N.B., Pérez-Aviles, D., Smith-Martin, C.M., Becknell, J.M., Aureli, F., Blanco, R., Calderón-Morales, E. et al. (2020) A catastrophic tropical drought kills hydraulically vulnerable tree species. *Global Change Biology*, 26(5), 3122–3133.
- Reich, P.B. (2014) The world-wide 'fast-slow' plant lant economics spectrum: a traits manifesto. *Journal of Ecology*, 102(2), 275–301.
- Rodriguez-Dominguez, C.M., CarinsMurphy, M.R., Lucani, C. & Brodribb, T.J. (2018) Mapping xylem failure in disparate organs of whole plants reveals extreme resistance in olive roots. New Phytologist, 218(3), 1025–1035.
- Ross, P.J. & Bristow, K.L. (1990) Simulating water movement in layered and gradational soils using the Kirchhoff transform. *Soil Science Society of America Journal*, 54(6), 1519–1524.
- Rowland, L., Martínez-Vilalta, J. & Mencuccini, M. (2021) Hard times for high expectations from hydraulics: predicting drought-induced forest mortality at landscape scales remains a challenge. New Phytologist, 230(5), 1685–1687.
- Sack, L. & Holbrook, N.M. (2006) Leaf hydraulics. *Annual Review Plant Biology* 571, 361–381.

- Scoffoni, C., Albuquerque, C., Brodersen, C.R., Townes, S.V., John, G.P., Bartlett, M.K., Buckley, T.N., McElrone, A.J. & Sack, L. (2017) Outside-xylem vulnerability, not xylem embolism, controls leaf hydraulic
- Scoffoni, C., Sack, L. & Ort, D. (2017) The causes and consequences of leaf hydraulic decline with dehydration. *Journal of Experimental Botany*, 68(16), 4479–4496.

decline during dehydration. Plant Physiology, 173(2), 1197-1210.

- Skelton, R.P., Anderegg, L.D., Diaz, J., Kling, M.M., Papper, P., Lamarque, L.J., Delzon, S., Dawson, T.E. & Ackerly, D.D. (2021) Evolutionary relationships between drought-related traits and climate shape large hydraulic safety margins in Western north American Oaks. Proceedings of the National Academy of Sciences United States of America, 118(10), e200887118.
- Skelton, R.P., Anderegg, L.D., Papper, P., Reich, E., Dawson, T.E., Kling, M., Thompson, S.E., Diaz, J. & Ackerly, D.D. (2019) No local adaptation in leaf or stem xylem vulnerability to embolism, but consistent vulnerability segmentation in a north American Oak. *New Phytologist*, 223(3), 1296–1306.
- Skelton, R.P., Brodribb, T.J. & Choat, B. (2017) Casting light on xylem vulnerability in an herbaceous species reveals a lack of segmentation. New Phytologist, 214(2), 561–569.
- Skelton, R.P., Brodribb, T.J., McAdam, S.A. & Mitchell, P.J. (2017) Gas exchange recovery following natural drought is rapid unless limited by loss of leaf hydraulic conductance: evidence from an evergreen woodland. New Phytologist, 215(4), 1399–1412.
- Skelton, R.P., Dawson, T.E., Thompson, S.E., Shen, Y., Weitz, A.P. & Ackerly, D. (2018) Low vulnerability to xylem embolism in leaves and stems of north American Oaks. *Plant Physiology*, 177(3), 1066–1077.
- Smith-Martin, C.M., Skelton, R.P., Johnson, K.M., Lucani, C. & Brodribb, T.J. (2020) Lack of vulnerability segmentation among woody species in a diverse dry sclerophyll woodland community. Functional Ecology, 34(4), 777–787.
- Song, J., Trueba, S., Yin, X.-H., Cao, K.-F., Brodribb, T.J. & Hao, G.-Y. (2022) Hydraulic vulnerability segmentation in compound-leaved trees: evidence from an embolism visualization technique. *Plant Physiology*, 189(1), 204–214. https://doi.org/10.1093/plphys/kiac034
- Sperry, J.S. (2003) Evolution of water transport and xylem structure. International Journal of Plant Sciences, 164(S3), S115–S127.
- Sperry, J.S., Adler, F., Campbell, G. & Comstock, J. (1998) Limitation of plant water use by rhizosphere and xylem conductance: results from a model. *Plant*, *Cell & Environment*, 21(4), 347–359.
- Sperry, J.S., Hacke, U., Oren, R. & Comstock, J. (2002) Water deficits and hydraulic limits to leaf water supply. *Plant, Cell & Environment*, 25(2), 251–263.
- Sperry, J.S. & Love, D.M. (2015) What plant hydraulics can tell us about responses to climate-change droughts. *New Phytologist*, 207(1), 14–27.
- Tai, X., Mackay, D.S., Anderegg, W.R., Sperry, J.S. & Brooks, P.D. (2017) Plant hydraulics improves and topography mediates prediction of aspen mortality in southwestern USA. New Phytologist, 213(1), 113–127.
- Trugman, A.T. (2022) Integrating plant physiology and community ecology across scales through trait-based models to predict drought mortality. *New Phytologist*, 234(1), 21–27.
- Trugman, A.T., Anderegg, L.D., Anderegg, W.R., Das, A.J. & Stephenson, N.L. (2021) Why is tree drought mortality so hard to predict? *Trends in Ecology & Evolution*, 36(6), 520–532.
- Tyree, M.T., Cochard, H., Cruiziat, P., Sinclair, B. & Ameglio, T. (1993) Drought-induced leaf shedding in walnut: evidence for vulnerability segmentation. *Plant, Cell & Environment*, 16(7), 879–882.
- Tyree, M.T., Davis, S.D. & Cochard, H. (1994) Biophysical perspectives of xylem evolution: is there a tradeoff of hydraulic efficiency for vulnerability to dysfunction? *IAWA Journal*, 15(4), 335–360.

- Tyree, M.T. & Dixon, M.A. (1986) Water stress induced cavitation and embolism in some woody plants. *Physiologia Plantarum*, 66(3), 397–405.
- Tyree, M.T. & Ewers, F.W. (1991) The hydraulic architecture of trees and other woody plants. *New Phytologist*, 119(3), 345–360.
- Tyree, M.T., Kolb, K.J., Rood, S.B. & Patiño, S. (1994) Vulnerability to drought-induced cavitation of riparian cottonwoods in Alberta: a possible factor in the decline of the ecosystem? *Tree Physiology*, 14(5), 455–466.
- Tyree, M.T. & Sperry, J.S. (1988) Do woody plants operate near the point of catastrophic xylem dysfunction caused by dynamic water stress?: answers from a model. *Plant Physiology*, 88(3), 574–580.
- Venturas, M.D., Todd, H.N., Trugman, A.T. & Anderegg, W.R. (2021) Understanding and predicting forest mortality in the Western United States using long-term forest inventory data and modeled hydraulic damage. New Phytologist, 230(5), 1896–1910.
- Villagra, M., Campanello, P.I., Bucci, S.J. & Goldstein, G. (2013) Functional relationships between leaf hydraulics and leaf economic traits in response to nutrient addition in subtropical tree species. *Tree Physiology*, 33(12), 1308–1318.
- Williams, A.P., Cook, B.I. & Smerdon, J.E. (2013) Rapid intensification of the emerging southwestern north American megadrought in 2020-2021. Nature Climate Change, 12(3), 1–3.
- Wolfe, B.T., Sperry, J.S. & Kursar, T.A. (2016) Does leaf shedding protect stems from cavitation during seasonal droughts? a test of the hydraulic fuse hypothesis. *New Phytologist*, 212(4), 1007–1018.
- Wu, M., Zhang, Y., Oya, T., Marcati, C.R., Pereira, L. & Jansen, S. (2020) Root xylem in three woody angiosperm species is not more vulnerable to embolism than stem xylem. *Plant and Soil*, 450(1), 479–495.
- Yang, S. & Tyree, M.T. (1994) Hydraulic architecture of Acer saccharum and A. rubrum: comparison of branches to whole trees and the contribution of leaves to hydraulic resistance. Journal of Experimental Botany, 45(2), 179–186.
- Zhu, S.-D. & Cao, K.-F. (2009) Hydraulic properties and photosynthetic rates in co-occurring lianas and trees in a seasonal tropical rainforest in southwestern China. *Plant Ecology*, 204, 295–304.
- Zhu, S.-D., Chen, Y.-J., Cao, K.-F. & Ye, Q. (2015) Interspecific variation in branch and leaf traits among three Syzygium tree species from different successional tropical forests. Functional Plant Biology, 42(4), 423–432.
- Zhu, S.-D., Liu, H., Xu, Q.-Y., Cao, K.-F. & Ye, Q. (2016) Are leaves more vulnerable to cavitation than branches? *Functional Ecology*, 30(11), 1740–1744.
- Zimmermann, M.H. (1978) Hydraulic architecture of some diffuse-porous trees. *Canadian Journal of Botany*, 56(18), 2286–2295.
- Zimmermann, M.H. (1982) Functional xylem anatomy of angiosperm trees. New Perspectives in Wood Anatomy, 59–70.
- Zimmermann, M.H. (1983) Xylem structure and the ascent of sap. Springer.

SUPPORTING INFORMATION

Additional supporting information can be found online in the Supporting Information section at the end of this article.

How to cite this article: Wilkening, J.V., Skelton, R.P., Feng, X., Dawson, T.E. & Thompson, S.E. (2023) Exploring within-plant hydraulic trait variation: a test of the vulnerability segmentation hypothesis. *Plant, Cell & Environment*, 46, 2726–2746. https://doi.org/10.1111/pce.14649